2010

Constraining the timescales of sediment sequestration associated with large woody debris using cosmogenic Be-7

G. B. Fisher

G. B. Fisher

F. J. Magilligan

J. M. Kaste
William & Mary, jmkaste@wm.edu

Recommended Citation

Fisher, G. B.; Fisher, G. B.; Magilligan, F. J.; and Kaste, J. M., Constraining the timescales of sediment sequestration associated with large woody debris using cosmogenic Be-7 (2010). *Journal of Geophysical Research-Earth Surface*, 115.
10.1029/2009JF001352

JOURNAL OF GEOPHYSICAL RESEARCH, VOL. 115, F01013, doi:10.1029/2009JF001352, 2010

Constraining the timescales of sediment sequestration associated with large woody debris using cosmogenic ^{7}Be

G. B. Fisher,[1,2] F. J. Magilligan,[3] J. M. Kaste,[4] and K. H. Nislow[5]

Received 13 April 2009; revised 25 August 2009; accepted 21 October 2009; published 31 March 2010.

[1] The beneficial ecogeomorphic functions associated with large woody debris (LWD) in fluvial environments are well documented and include positive sediment impacts such as channel margin sequestration, increased substrate heterogeneity, and decreased channel embeddedness, as well as numerous secondary benefits such as nutrient retention and increased habitat heterogeneity. Despite an extensive literature documenting such positive sediment attributes of LWD in forested channels, a quantitative analysis of in-channel sediment storage times associated with channel obstructions has traditionally been difficult to assess. In this study along a 9 km stretch of the Ducktrap River in coastal Maine we present a novel application of fallout cosmogenic ^{7}Be ($t_{1/2}$ = 53 days) coupled with a constant initial activity (CIA) sediment aging model to quantitatively assess transitional bed load storage times in bars associated with in-channel obstructions (LWD and boulders). We find that reach-scale variability in unit stream power and LWD frequency affect sediment storage times, with transport-limited reaches providing longer-term sediment sequestration (generally > 100 days) associated with in-channel obstructions than supply limited ones (<100 days). Estimates of sediment baraccumulation rates also varied between reaches from 0.2 g cm^{-2} d^{-1} in the supply limited reach to 0.7 g cm^{-2} d^{-1} in the transport-limited reach. Last, greater frequency of sites, increased sediment volumes and storage times, and naturally viable recruitment mechanisms for LWD in forested channels document its superior ecogeomorphic function when compared to boulders in this study, even in the Ducktrap river, where twentieth century logging has greatly reduced the size, frequency, and geomorphic efficacy of in-channel wood. This study has implications for channel restoration efforts and documents a novel application of ^{7}Be and CIA methodology to constraining transitional bed load storage times in the fluvial environment.

Citation: Fisher, G. B., F. J. Magilligan, J. M. Kaste, and K. H. Nislow (2010), Constraining the timescales of sediment sequestration associated with large woody debris using cosmogenic ^{7}Be, *J. Geophys. Res.*, *115*, F01013, doi:10.1029/2009JF001352.

1. Introduction

[2] Considerable literature on large woody debris (LWD) verifies its ecological, hydrologic, and geomorphic importance in regulating and restoring (in anthropogenically modified landscapes) sediment dynamics and natural processes in forested watersheds. Large woody debris provides numerous ecogeomorphic functions such as cover [*Montgomery et al.*, 2003], interstitial space [*Manners et al.*, 2007], increased habitat complexity [*Montgomery et al.*, 2003] and sediment storage [*Bilby*, 1981; *Keller et al.*, 1995; *Lancaster et al.*, 2001], pool formation [*Montgomery et al.*, 1995; *Wohl et al.*, 1997], and enhances variability in channel architecture and flow regimes [*Keller and Swanson*, 1979; *Lisle*, 1986]. In addition, increased hydraulic roughness and flow resistance by LWD [*Manga and Kirchner*, 2000] promote larger and more frequent sites of sediment deposition, as well as the mobilization of fine-grained material from thalweg to channel margin sites through the creation of dynamic eddies and bars [*Rathburn and Wohl*, 2003; *Daniels and Rhoads*, 2004]. These functional characteristics of LWD in turn diminish embeddedness, provide vital nutrient storage, and help regulate excess sediment flux in disturbed systems.

[3] Despite the extensive body of literature aimed at understanding the relationship between fine-grained sediment, channel obstructions (LWD, boulders, etc.), and hydrologic

[1]Department of Earth Sciences, Dartmouth College, Hanover, New Hampshire, USA.
[2]Department of Earth Science, University of California, Santa Barbara, California, USA.
[3]Department of Geography, Dartmouth College, Hanover, New Hampshire, USA.
[4]Department of Geology, College of William and Mary, Williamsburg, Virginia, USA.
[5]Northern Research Station, U.S. Department of Agriculture, U.S. Forest Service, University of Massachusetts, Amherst, Massachusetts, USA.

0148-0227/10/2009JF001352

dynamics, several unknowns remain. While numerous studies have focused on quantifying watershed-scale particle residence times or suspended load transport rates [*Malmon et al.*, 2003; *Nistor and Church*, 2005; *Dosseto et al.*, 2006], there is a limited understanding of in-channel, transitional bed load (63 μm to 2mm) storage times related to an array of channel features. Previous studies have utilized scour chains to quantify transitional bed load storage times in pools in the Northwest and found relatively rapid turnover rates during subbankfull discharges, indicating frequent scour conditions [*Lisle*, 1979; *Lisle and Hilton*, 1999]. However, no work to our knowledge has sought to quantify the storage time of transitional bed load sediment associated with in-channel obstructions (i.e., LWD, boulders, etc.) where flow velocities are generally attenuated (by increased flow resistance) throughout normal flow regimes and thus storage times may be considerably longer term compared to open pools or thalweg deposition. It is therefore valuable to understand the relative contribution of channel obstructions in the context of larger-scale sediment dynamics in order to enhance future studies of sediment budgets and transport regimes, watershed-scale residence times, and ecogeomorphic and channel restoration dynamics in forested watersheds.

[4] In this study we present a novel technique for using fallout cosmogenic ^{7}Be ($t_{1/2}$ = 53.3 days) to answer two major research questions. First, what is the storage time of transitional bed load sediment associated with in-channel obstructions and how does it vary by the type of obstruction (LWD or boulder)? Second, to get at the processes of sediment storage, how do reach-scale characteristics such as slope, sediment transport regime, and LWD frequency affect the timescales of sediment storage behind such obstructions? In addition, we compare in-channel and low-flow emergent channel bar sediment storage times constrained by ^{7}Be and stratigraphic estimates to (1) gain an enhanced understanding of the timescales involved with LWD and boulder sediment sequestration and (2) illuminate the potential sediment impacts involved with wood loss/additions in disturbed watersheds. Last, we provide an alternative methodology for comparing and reporting radionuclide activities using a specific surface area normalized methodology and detail the promises and caveats of the ^{7}Be sediment storage aging technique.

2. Cosmogenic ^{7}Be in the Fluvial Environment

[5] ^{7}Be is a naturally occurring fallout radionuclide produced by cosmic ray spallation of nitrogen and oxygen, predominantly in the upper atmosphere [*Lal et al.*, 1958]. Once formed, it has a high affinity for atmospheric aerosols, with subsequent deposition occurring disproportionately through wet fallout, with lesser dry deposition [*Olsen et al.*, 1985; *Wallbrink and Murray*, 1994]. While regional and temporal variations in ^{7}Be deposition may be substantial, constraints can be achieved by measuring reference soils, using extensive sampling strategies, or by monitoring precipitation/atmospheric fallout [*Blake et al.*, 2002]. Once ^{7}Be reaches the soil surface, the charged molecule strongly [*You et al.*, 1989] adsorbs to particle surfaces with reported distribution coefficients (K_d) of 10^5–10^6 (between solid and liquid phases) and is retained in the upper few cm of soil [*Hawley et al.*, 1986; *Wallbrink and Murray*, 1996; *Kaste et al.*, 2007]. Due to this strong preferential adsorption of the ^{7}Be molecule to particle surfaces, exposed sediment accumulates ^{7}Be activity through continuous fallout dosing while water typically remains devoid of activity. Therefore, once a ^{7}Be tagged particle is eroded off of the landscape and becomes submerged in a water body (river, lake, ocean, etc.) it ceases to accumulate ^{7}Be activity and the activity signal becomes dominated instead by radioactive decay. If proper constraints can be placed on the initial activity at the time of deposition, then the particle activity can be used to calculate the storage/deposition time using exponential decay theory [*Bonniwell et al.*, 1999].

[6] While numerous studies have utilized fallout radionuclides to study sediment transport processes [*Bonniwell et al.*, 1999; *Blake et al.*, 2002; *Matisoff et al.*, 2005; *Whiting et al.*, 2005], most studies have focused solely on suspended sediment transport with two exceptions. *Salant et al.* [2007] utilized ^{7}Be/^{210}Pb dynamics of sediment originating behind a dam to infer transitional bed load transport velocities associated with seasonal dam releases in New England, while *Svendsen et al.* [2009] utilized ^{7}Be systematics to understand the magnitude and type of impact (negative/positive) tributary junctions have on regulated river sediment regimes and biotic communities. These studies, to our knowledge, represent the only literature on transitional bed load dynamics using fallout radionuclides, and only recently has the valid detection of radionuclides on sand size particles been demonstrated [*Magilligan et al.*, 2008b].

3. Study Area and Geologic Setting

[7] Located on the central coast of Maine on the western margin of Penobscot Bay (Figure 1), the Ducktrap River watershed (94.2 km^2) is dominated by Quaternary fine-grained (primarily sand) surficial deposits of till (93%) and postglacial retreat transgressional marine facies (3.7%), with bedrock exposed in only 3.3% of the total watershed (Table 1). The Ducktrap River receives average monthly precipitation of approximately 10 cm +/− 1.48 (1 σ) and has a bimodal flood regime (Q_2 = 14.3 m^3 s^{-1}) with high flows occurring as snowmelt in late spring or coincident with large rain events in the late fall [*Magilligan and Graber*, 1996]. Channel substrate size is mixed ranging from fine to medium sand dominated beds in lower-gradient sections to cobble/boulder dominated in higher-gradient sections.

[8] Several attributes of the Ducktrap watershed make it well suited for studying relationships between sediment storage times and channel features using cosmogenic ^{7}Be. First, the existence of an extensive LWD database collected in August 2005 provides time constraints on wood location/stability, allowing calculations of sediment storage times to be representative of flow characteristics and not related to wood mobility/stability. If this were not the case, any sediment bar associated with LWD could simply be recording the time that the log has been in place and/or a prior hydraulic regime. Second, the relict glacial history of the region has formed large ponds where the main stem Ducktrap and several tributaries all initiate, providing a sink for any sediment shed from the steeper upland hillslopes (Figure 1) and effectively decoupling the hillslopes from

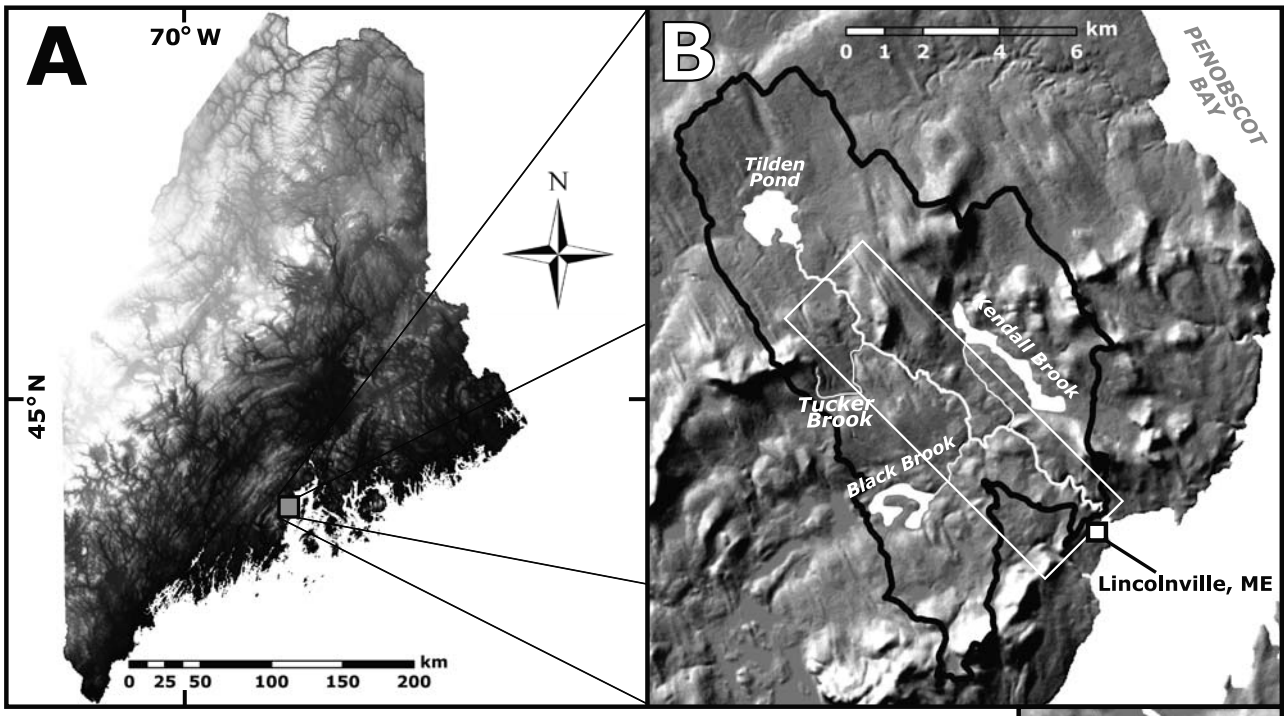

C

LWD	Emergent	Thal.	Boulder	Site ID (River km)
		T-11.6		11.6
TB-LWD	TB-EB			Tucker Brook (10.8)
LWD-10.7	EB-10.7			10.7
		T-9.1	B-9.1	9.1
	EB-8.8	T-8.8		8.8
LWD-8.4		T-8.4		8.4
		T-7.9	B-7.9	7.9
LWD-7.5	EB-7.5	T-7.5		7.5
LWD-7.45				7.45
LWD-7.4				7.4
LWD-7.2	EB-7.2	T-7.2		7.2
		T-6.9	B-6.9	6.9
LWD-6.0	EB-6.0	T-6.0		6.0
		BB-T		Black Brook (5.5)
		T-5.3	B-5.3	5.3
LWD-5.1	EB-5.1	T-5.1		5.1
		KB-T		Kendall Brook (4)
		T-3.0		3.0

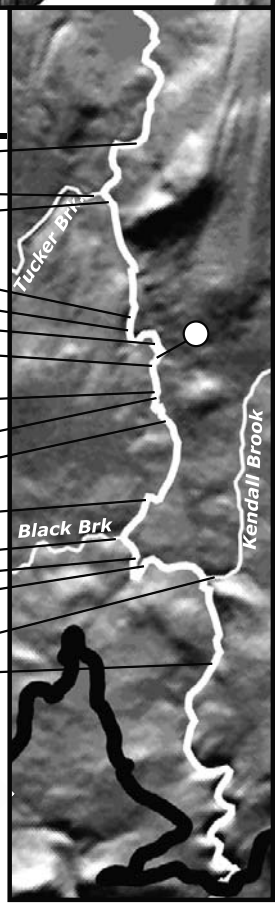

○ = USGS Gaging Station

0 1 2 4 km

N

Figure 1. (a) Digital elevation model (DEM) map of Maine, (b) hill shade map of the Ducktrap watershed, and (c) sample locations and types along the study reach with site identification by distance from the mouth of the Ducktrap River. LWD, submerged sediment bar associated with large woody debris; EB, emerged sediment bar; B, submerged sediment bar associated with a boulder; T, submerged thalweg sample. Tributary samples are identified by tributary abbreviation followed by sample type. Note the location of Tucker Brook, as it is the main transitional bed load sediment source to the study reach.

Table 1. River and Wood Characteristics for the Ducktrap River Obtained From DEM Analysis and Field Surveys[a]

	Value
Ducktrap River characteristics	
Watershed area	94.2 km^2
River length (from Tilden Pond)	15.6 km
2 year recurrence interval discharge	14.3 $m^3 s^{-1}$
Average gradient	0.45%
Maximum reach averaged gradient	0.94%
Average sinuosity	1.37
Average channel width	10.2 m
Reach average channel width at outlet of Tilden Pond	8 m
Reach average channel width at the Ducktrap River mouth	14 m
Ducktrap River wood characteristics	
Total pieces sampled ≥ 10 cm in diameter	1586
Mean piece diameter	21 cm (±8 cm)
Mean piece length	5 m (±3.7 m)
Number of pieces < 20 cm in diameter (average pieces km^{-1})	800 (51.3 pieces km^{-1})
Number of pieces ≥ 20 cm and <50 cm in diameter (average pieces km^{-1})	766 (49.1 pieces km^{-1})
Number of pieces ≥ 50 cm in diameter (average pieces km^{-1})	20 (1.28 pieces km^{-1})
Total wood volume	23 $m^3 km^{-1}$
Percent of wood volume found in low-flow channel	46%
LWD oriented parallel to flow	31.5%
LWD oriented perpendicular to flow	18.9%
LWD oriented subperpendicular to flow with base upstream	35.6%
LWD oriented subperpendicular to flow with base downstream	14.0%
LWD associated with pool formation	12.6%
LWD associated with sediment storage	14.4%

[a]Analysis and field surveys were conducted by the Maine Atlantic Salmon Commission following the protocols outlined by *Schuett-Hames et al.* [1999]. LWD frequency is considerably low and generally lacking in large pieces and perpendicular orientations [*Magilligan et al.*, 2008a]. Likewise, LWD associated with pool formation and sediment storage is negligible.

the main stem. In contrast, Tucker Brook receives constant sediment inputs from mass wasting processes in its higher reaches and, due to the lack of ponds in its drainage basin, acts as the dominant sediment source to the study reach. This basic assumption is further validated by field observations documenting both a lack of fine sediment in the Ducktrap River upstream of the junction with Tucker Brook and the presence of considerable transitional bed load sediment both within Tucker Brook as well as downstream of the junction with the Ducktrap River. Third, the presence of well-armored banks and low-gradient, well-vegetated floodplains and hillslopes along the study reach prevent major inputs to ^{7}Be activities from lateral channel migration, bank collapse, and/or rilling. Last, the presence of two distinct transport regimes (transport and supply limited) [cf. *Montgomery and Buffington*, 1997], identifiable in the field and by topographic analysis, allows the comparison of sediment storage timescales associated with channel obstructions across variable slopes and entrainment thresholds. It is important to note that in this paper we define transport limited and supply limited with respect to transitional bed load mobility, where thalwegs are generally devoid of transitional bed load at subbankfull flows in the supply-limited reach and quite pervasive in the thalweg of the transport-limited reach. This simplistic watershed structure provides a well-controlled study system where transitional bed load material first enters through Tucker Brook and then alternates between exposed depositional sites (emergent bars, accumulating ^{7}Be activity) and submerged ones (submerged bars, decaying ^{7}Be activity) along the study reach, ultimately allowing simplification in delineation of initial ^{7}Be activities and sediment storage model assumptions.

4. Methods

4.1. Site Locations and Sediment Sampling Strategy

[9] In-channel sediment bars associated with LWD (9 total) and boulders (4 total) as well as emergent bars (7 total (represent longer-term storage)) and thalweg grab samples (14 total (to represent the activities of sediment currently/recently in transport)) were taken between 22 July and 16 August 2006 within the Ducktrap watershed (Figures 1 and 2). Submerged sediment bars downstream of LWD ≥ 20 cm in diameter and perpendicular to flow were located prior to fieldwork using an extensive wood survey GIS database collected in August 2005 by the Maine Atlantic Salmon Commission (Figure 3 and Tables 1 and 2). Large woody debris sites from the GIS database were subsequently located in the field (to assure wood had been stable for >1 year) and an array of sediment bars were sampled using a corer of our own design (26 cm diameter aluminum tube with 5 cm increment slots for sheet metal dividers) in 5 cm depth bins until the coarse channel bed (usually gravel) was reached (Figure 2). Sediment bars associated with boulders were sampled in the same way, while emergent bars were sampled at 5 cm depth increments until the water surface was reached. At each location detailed sketches, measurements, and observations were taken in order to supplement isotopic analysis (Table 2). All LWD and boulder submerged sediment bars were revisited at base flow levels (~0.11 $m^3 s^{-1}$ at the gauge) to assure that they had not been exposed to any direct wet or dry atmospheric deposition, which would overprint and destroy the submerged signal of decay. Sites were also revisited in the summer of 2007 to verify the stability of wood at sample locations in order to further validate site selection and results.

4.2. Radionuclide and Sediment Surface Area Measurements

[10] After field collection, alluvial sediments were sieved to between 63 μm and 2 mm in size and organics, soluble coatings, and flocculated fine particles were agitated and removed to ensure the activity signal being measured was solely from the transitional bed load fraction and not overprinted by organic material (which generally have much higher activities due to atmospheric scavenging). The general lack of fine-grained and organic material observed in and removed from the samples, along with recent experimental results that demonstrate the efficacy of 2–4 mm diameter crushed diorite in retaining >90% of the atmospherically delivered ^{7}Be over multiple precipitation events, gives us great confidence that the signal being measured results entirely from the transitional bed load fraction [*Magilligan et al.*, 2008b]. Sample activities (Bq kg^{-1}) of ^{7}Be were

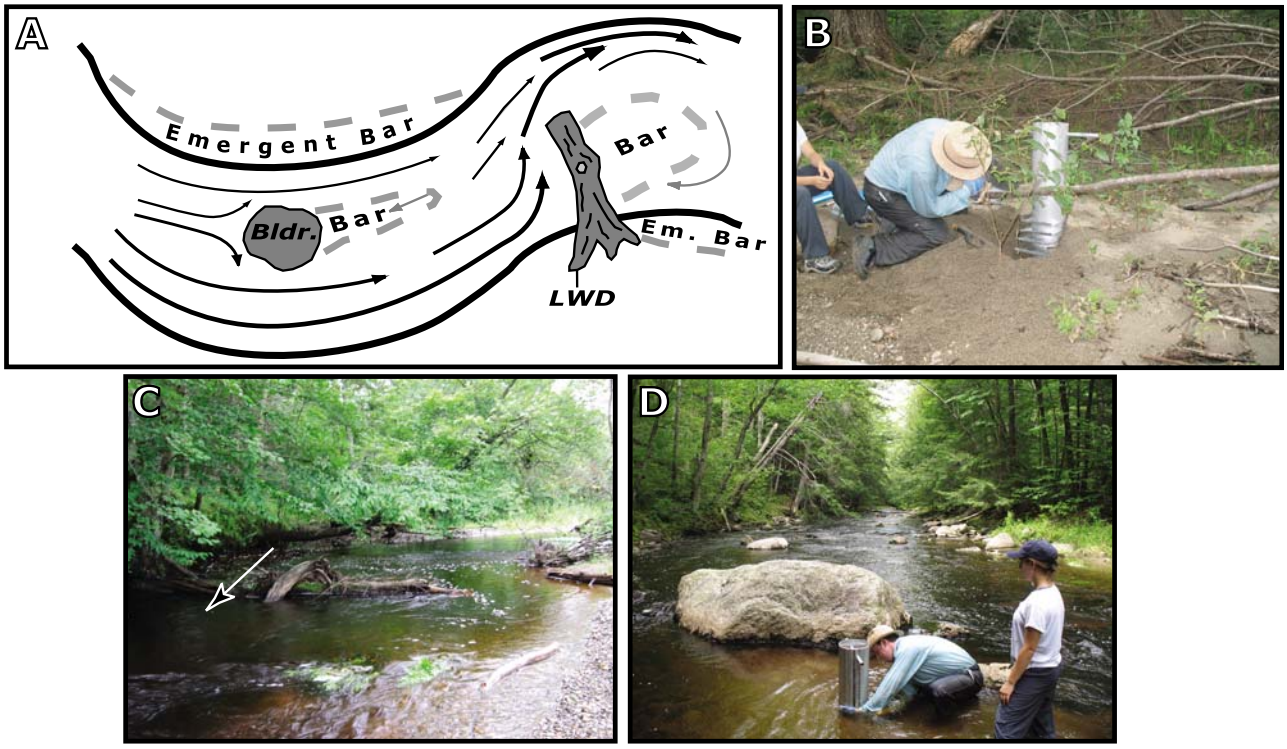

Figure 2. (a) Conceptual model of sediment bar location and formation with respect to in-channel and emergent channel features (LWD, boulders, sinuosity, etc.) along with generalized flow vectors. Photographs of (b) the coring device and metal slots used to partition 5 cm depth samples, (c) perpendicular woody debris (LWD-10.7) and associated depositional eddy (arrow) where the core was taken (downstream flow is also in the direction of the arrow), and (d) sediment storage associated with a boulder (B-9.1) in the supply-limited reach.

then measured using a high-purity germanium detector via gamma counting at 478 keV. Activities were calculated by correcting for sample mass, decay since collection, counting time, detector and photon efficiencies, and a small peak interference with actinium-228 [*Kaste et al.*, 2002]. Analytical error associated with gamma counting is a function of the total number of photons detected and uncertainty in modeling the background in the 474–484 keV region. Cosmogenic ^{7}Be activities in this study had uncertainties ranging from 5% to 15% with a mean of 8.8% and a median of 8.7%. Analytical detection limits were calculated to be 0.6 Bq kg^{-1} at the 2 σ level for a 100 ks count time to separate background noise from actual ^{7}Be signal.

[11] Constraining particle size variability is also important for properly comparing radionuclide activities across samples. Previous studies have demonstrated virtually indistinguishable partition coefficients for ^{7}Be between sand, silt, and mud (10^{5} +/− 15%) [*You et al.*, 1989] as well as increased adsorption ability with increased surface area [*He and Walling*, 1996a], potentially producing increased activities per given sample weight. A host of techniques have been developed to account for variability in particle surface areas from using complex multinuclide ratios and/or ^{210}Pb proxies [*Bonniwell et al.*, 1999; *Matisoff et al.*, 2005; *Salant et al.*, 2007] to normalization by clay content [*Aalto et al.*, 2003]. In order to provide a more direct analysis of grain size and to avoid potential problems of normalizing by ^{210}Pb (such as the contribution of ^{222}Rn in groundwater, complicated activity inheritance histories, and the relative contributions of atmospheric ^{210}Pb and ^{210}Pb due to the decay of ^{226}Ra in the local regolith), specific sediment surface areas (SSA) for all samples were measured. Samples were analyzed using the BET method, a standard technique that measures the adsorption of gas onto mineral surfaces to quantify surface area [*Brunauer et al.*, 1938; *Gregg and Sing*, 1982], and measured on a Micromeritics FlowSorb III 2305 surface area analyzer with a 30% N_2/70% He gas mixture and a Micromeritics DeSorb III 2300A three station outgassing unit to increase throughput of samples. Accuracy of the instrument is +/−3% with reproducibility of +/−0.5%. Sample specific surface areas (hereafter referred to as SSA) were calculated in m^{2} kg^{-1} and then ^{7}Be activities (Bq kg^{-1}) were divided by SSA to yield Bq m^{-2}. All ^{7}Be activities are reported here in units of mBq m^{-2} SSA (hereafter mBq m^{-2}). While we acknowledged that sorption site density may change with compositional variations, the method does provide a direct and accurate alternative for standardizing activities across samples, and is invaluable in instances where ^{210}Pb systematics are complicated or poorly constrained. In our system, however, high correlation between specific surface area normalized and ^{7}Be/^{210}Pb$_{total}$ values ($R^2 = 0.81$) documents the efficacy of both techniques (Figure 4), with radionuclide ratios proving more time efficient in the end because specific surface area analyses are not required.

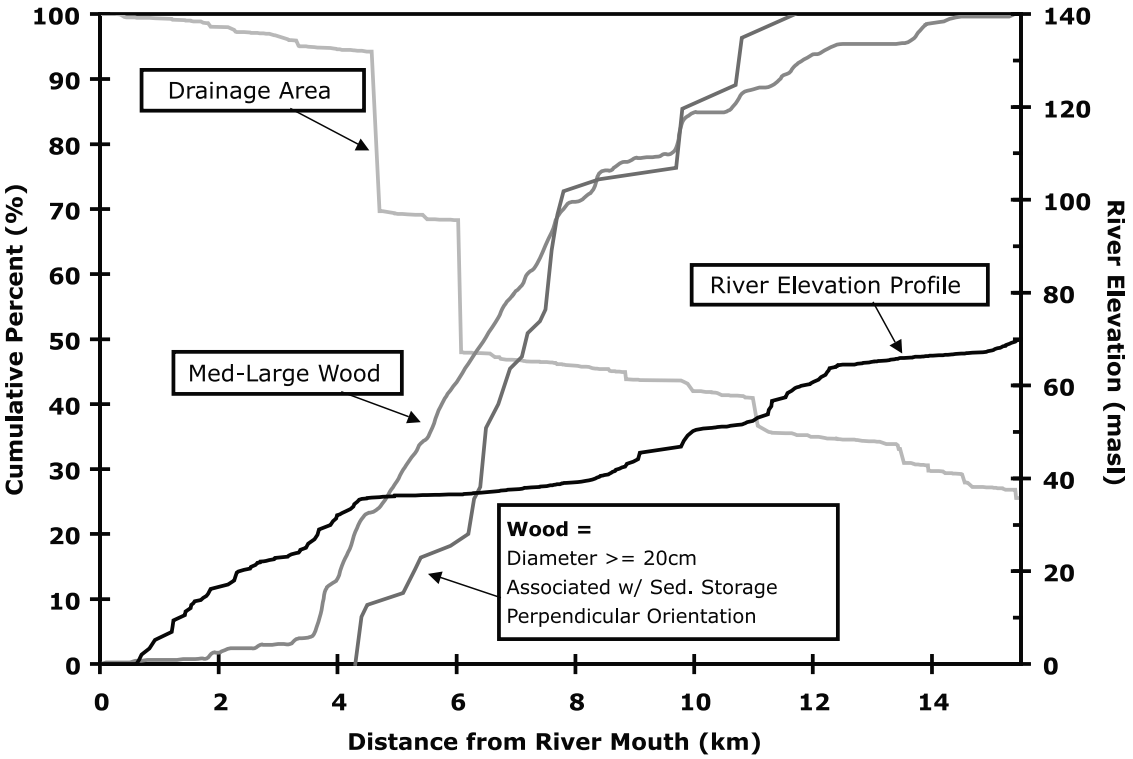

Figure 3. Graph of the Ducktrap River elevation profile with cumulative percent drainage area, cumulative percent of medium and large wood (≥20 cm diameter) (n = 786), and cumulative percent of wood that meets the study sampling criteria (wood ≥ 20 cm in diameter with associated sediment storage and perpendicular orientation to flow) (n = 27). Longitudinal profile was extracted from a 10 m DEM and then filtered using a five-point moving average filter.

Table 2. Site Characteristics for Ducktrap River Samples[a]

	Distance From River Mouth (m)	Orientation	Diameter	Log Length (cm)	Depth to Submerged Bar From Water or Depth to Water From EB (cm)	Sediment Wedge Orientation in Relation to Banks[b]	River Location	Approximate Sediment Wedge Volume (m^3)
LWD								
TB-LWD	10.8	perpendicular	25 cm	300	15	parallel	RL	0.20
LWD-10.7	10.7	perpendicular	30 cm	400	50	parallel	C/RR	0.15
LWD-8.4	8.4	perpendicular	45 cm	450	24	perpendicular	C/RR	0.47
LWD-7.5	7.5	perpendicular	26 cm	850	24	parallel	C/RR	1.03
LWD-7.45	7.45	perpendicular	21 cm	350	47	parallel	RR	1.22
LWD-7.4	7.4	perpendicular	20 cm	425	32	parallel	RL	2.16
LWD-7.2	7.2	perpendicular	35 cm	575	10	parallel	RR	0.80
LWD-6.0	6.0	perpendicular	22 cm	700	12	parallel	C/RR	2.21
LWD-5.1	5.1	perpendicular	35 cm	1800	38	parallel	C/RL	2.59
Emerged bars								
TB-EB	10.8	perpendicular	25 cm	300	20	parallel	RL	0.47
EB-10.7	10.7	perpendicular	20 cm	300	20	parallel	RL	0.31
EB-8.8	8.8	perpendicular	39 cm	1600	29	parallel	RR	1.47
EB-7.5	7.5	NA	NA	NA	40	parallel	RL	14.14
EB-7.2	7.2	perpendicular	35 cm	575	30	parallel	RR	9.42
EB-6.0	6.0	NA	NA	NA	25	parallel	RL	7.07
EB-5.1	5.1	NA	NA	NA	10	parallel	RL	0.63
Boulder								
B-9.1	9.1	perpendicular	2 m	NA	15	parallel	C	2.77
B-7.9	7.9	parallel	1 m	NA	38	parallel	C	0.37
B-6.9	6.9	perpendicular	1 m	NA	33	parallel	C	0.39
B-5.3	5.3	perpendicular	1.5 m	NA	21	parallel	C	0.88

[a]Log orientation and diameter are given for LWD and emerged bar profiles, and boulder orientation and diameter of the long axis are given for boulder profiles. NA, not applicable.
[b]Sediment wedge orientation values are for the long axis.

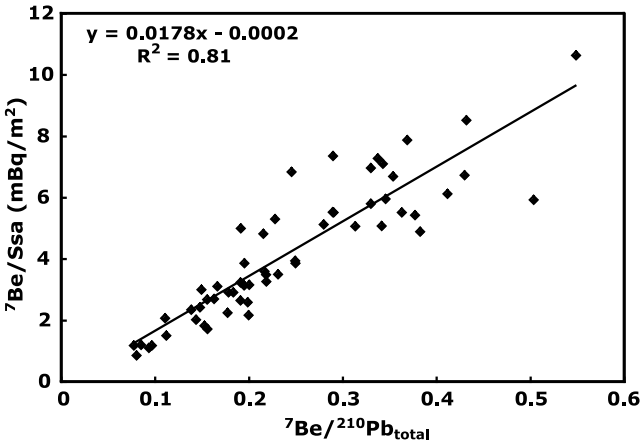

Figure 4. Plot of ^{7}Be/SSA (mBq m^{-2}) against ^{7}Be/^{210}Pb$_{total}$ with associated trend line and R^2 value. SSA refers to the specific sediment surface area.

4.3. Sediment Storage Time Theory, Model, and Assumptions

[12] A number of techniques have recently been developed to quantify sediment dynamics in fluvial environments using fallout radionuclides [*Bonniwell et al.*, 1999; *Fitzgerald et al.*, 2001; *Walling et al.*, 2008]. These models are always based on the assumption that the radioisotopes adsorb strongly and irreversibly to sediment particles, and with appropriate treatment of the data, the constant decay rate of a nuclide can be used as a "clock" as changes in radionuclide concentration can be related to particle residence times [e.g., *Feng et al.*, 1999; *Bonniwell et al.*, 1999] or burial and sedimentation rates [*Aalto et al.*, 2003; *Appleby and Oldfield*, 1992]. In this study a constant initial activity (CIA) exponential decay model is used to calculate storage times:

$$\ln(A/A_0)/-\lambda = t \quad (1)$$

where A is the observed activity of the sample (mBq m^{-2}), A_0 is the initial activity at the time of deposition (mBq m^{-2}), λ is the decay constant of ^{7}Be (0.013 d^{-1}), and t is the storage time (in days). The CIA model was chosen for several reasons: (1) it does not require radioactive equilibrium or a constant rate of sediment supply, which is virtually impossible given the complex nature of fluvial sediment dynamics at the timescales that ^{7}Be is applicable; (2) it can be utilized in fluvial systems devoid of fine sediments (<63 μm); and (3), the temporal error associated with our technique (~53 days) is reasonably small with respect to the timescales that we are trying to resolve (hundreds of days). In this study we bracket initial activities and subsequent storage time calculations by defining a range of values using one standard deviation above and below the mean of thalweg and emergent bar surface sample activities (assumed source of material of depositional bars) (Figures 5 and 6). We also approximate an "optimal" initial activity that accounts for longitudinal variability and acts as a best estimate of the initial activity of each site based on the adjacent thalweg and emergent bar surface sample activities. Last, sampling in 5 cm depth bins averages out any extreme smaller-scale ^{7}Be variability associated with individual layers and/or lenses.

[13] Major assumptions of our study (justified by both field and radionuclide analysis) are (1) that Tucker Brook represents the main sediment source for the study reach, where any accumulation of ^{7}Be occurs through wet atmospheric deposition in the top 5 cm [*Kaste et al.*, 2002] of emergent bars along the channel margin and not through external inputs (rilling, landsliding, overland flow, etc.), and (2) that the sediment being deposited on in-channel bars originates from mobilization and subsequent deposition of thalweg and emergent bar surface sediments. This second assumption holds especially true in the supply-limited section where thalweg sediment storage times are negligible and can thereby be treated as recently mobilized exposed bar sediments deposited on the falling limb of the last discharge event. In addition, field observations indicate much greater sediment exposed on emergent bars (~95%) than in the channel. In the transport-limited section we make the same assumption and justify it by the presence of consistent activity values between adjacent thalweg and emergent bar surface samples along the study reach ($\ll$1 half-life of variability) (Figures 5 and 6). However, we do acknowledge that longer-term thalweg storage times (substantial decay) as well as greater volumes of submerged sediment (dilution effects) may create greater errors associated with the delineation of initial activities in such transport-limited regimes. Despite this potential complication, we are quite confident that our careful treatment of initial activity variability both statistically and longitudinally along the study reach yields a robust and well-constrained framework for calculating sediment storage times associated with channel obstructions and showcases the potential of a novel application of both ^{7}Be and the CIA model to a fluvial system.

5. Results

5.1. Thalweg and Emergent Bar Surface (0–5 cm) Activities and CIA Constraints

[14] Thalweg and emergent bar surface samples (0–5 cm) throughout the watershed were used to constrain initial ^{7}Be activity ranges for sediment being deposited on in-channel bars associated with LWD and boulders (Figures 5 and 6 and Table 3). A mean value of 5.12 mBq m^{-2} with upper and lower 1 σ values of 7.72 mBq m^{-2} and 2.52 mBq m^{-2} defines the range of initial activity values applied in our storage age calculations (Figure 5). These initial activities, along with analytical detection limits, dictate the sensitivity of the model and yield detectable timescales of ~2 half-lives (~106 days) for the lower 1 σ value, ~3 half-lives (~160 days) for the mean, and ~4 half lives for the upper 1 σ value (~210 days). Throughout the study reach thalweg and emergent bar surface samples closely track one another ($\ll$1 half-life) further validating their connectivity and use as proxies for initial sediment activities in depositional bars (Figure 6).

[15] Three main activity domains exist in the emergent bar surface and thalweg samples along the study reach. The first domain begins at Tucker Brook where sediment is fluxed into the transitional bed load starved Ducktrap River and then deposited on emergent bars, increasing ^{7}Be activities from Tucker Brook to site T-9.1 (Figure 5). This domain is

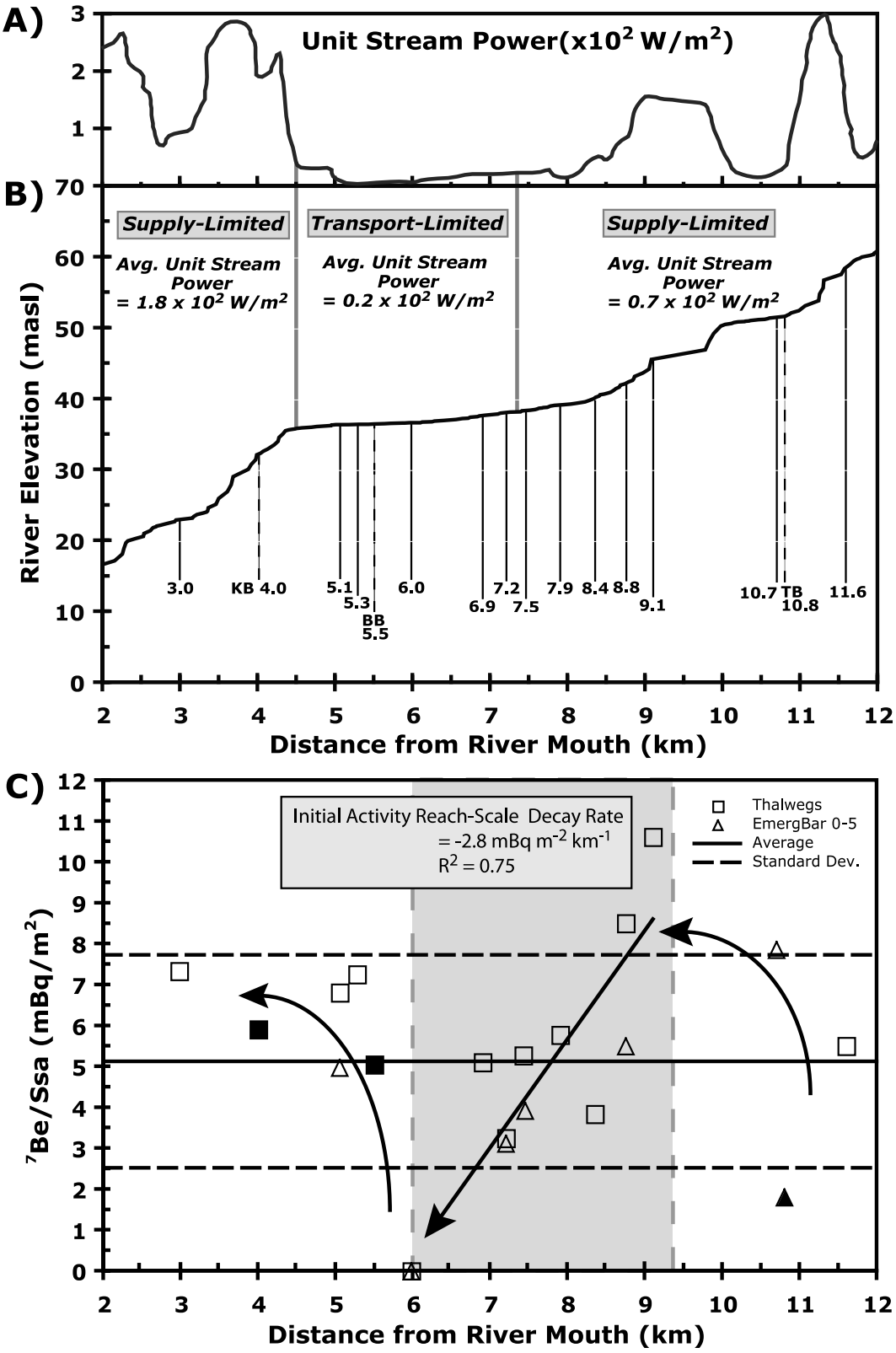
A)
Unit Stream Power(x10² W/m²)
B)
Supply-Limited
Avg. Unit Stream Power = 1.8 x 10² W/m²
Transport-Limited
Avg. Unit Stream Power = 0.2 x 10² W/m²
Supply-Limited
Avg. Unit Stream Power = 0.7 x 10² W/m²
River Elevation (masl)
3.0
KB 4.0
5.1
5.3
BB 5.5
6.0
6.9
7.2
7.5
7.9
8.4
8.8
9.1
10.7
TB 10.8
11.6
Distance from River Mouth (km)
C)
Initial Activity Reach-Scale Decay Rate = -2.8 mBq m⁻² km⁻¹
R² = 0.75
Thalwegs
EmergBar 0-5
Average
Standard Dev.
⁷Be/Ssa (mBq/m²)
Distance from River Mouth (km)

Figure 5

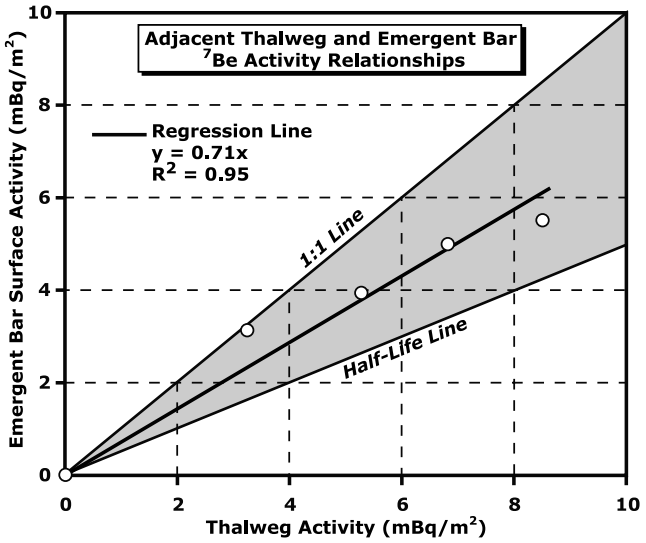

Figure 6. Regression of adjacent thalweg and emergent bar surface sample activities used to validate their similarity and use in constraining initial activities values. Data indicate close similarity between thalweg and emergent bar surface activities with deviation of only ~0.5 half-lives overall (~26 days).

characterized by diminished slopes and calculated unit stream power values directly downstream of the junction with Tucker Brook, leading to prolonged sediment exposure times on emerged bars and increased ^{7}Be activities. In addition, the low activity of the incoming sediment from Tucker Brook can be explained by a much smaller channel geometry (max channel width of ~3 m), which allows overhanging vegetation to scavenge ^{7}Be and diminish sediment exposure to ^{7}Be fallout on low-flow emergent channel bars.

[16] The second domain is characterized by a linear decrease in activities from site T-9.1 to river kilometer 6.0 (−2.8 mBq m^{-2} km^{-1}), which is attributed to greater in-channel grain submersion/decay as compared to exposure/increase in ^{7}Be on emergent bars. A simple reach-scale exponential decay calculation (domain distance/decay time) incorporating no complex sediment mixing or exposure/inundation history yields an upper limit transitional bed load transport rate of ~16 m d^{-1}, a value which is quite reasonable with respect to both experimental and field studies of bulk and transitional bed load transport rates in similar environments [e.g., *Pyrce and Ashmore*, 2003; *Salant et al.*, 2007]. While initial activity characterization would prove simpler with consistent values throughout the study reach, the presence of a consistent decreasing trend in the second domain allows for proper adjustment of initial activities with distance downstream (i.e., 7.72 mBq m^{-2} is more appropriate at river kilometer 9 than kilometer 7). It should also be noted that we assume that the observed trends in thalweg and emergent bar surface activities throughout the study reach are time invariant at the timescales of concern (~210 days) and that initial activities are a function of distance along the river (i.e., sediment is always dead by the time it reaches river kilometer 6.0). Last, the third domain is characterized by increased thalweg and emergent bar surface activities (associated with higher-activity sediments from Kendall and Black Brooks), increased unit stream power and channel slopes (Figure 5), and greater emergent bar transitional bed load storage compared to in-channel storage, similar to the first domain.

5.2. Activities and Storage Times of Submerged Bars Associated With In-Channel Obstructions

[17] Eight submerged sediment bars associated with LWD were cored along the main stem Ducktrap River at kilometers 10.7, 8.4, 7.5, 7.45, 7.4, 7.2, 6.0, and 5.1 as well as one on the lowest reach of Tucker Brook tributary (TB-LWD), located 10.8 km upstream of the Ducktrap River mouth (Figures 1 and 8). Additionally, four submerged sediment bars associated with boulders were sampled at river kilometers 9.1, 7.9, 6.9, and 5.3 (Figures 1 and 9). LWD and boulder sediment cores taken from the main stem Ducktrap River exhibit three types of activity profiles (Figure 7) and fall into two dominant transport regimes (supply and transport limited) delineated by field observations and slope based proxies of sediment mobility (Figure 5). The first profile type is single event deposition as seen in TB-LWD, LWD-10.7, LWD-8.4, and LWD-7.45, all found in the supply-limited reach (Figures 7 and 8 and Table 3). TB-LWD has slightly decreasing activity with depth, most likely representing a single depositional event, and a basal sample lacking ^{7}Be activity. The data indicate that TB-LWD was previously scoured to the 20 cm depth basal sample, followed by a single depositional event of sediment with homogenous ^{7}Be activity. In contrast, LWD-10.7 and LWD-8.4 are characterized by increasing activity with depth. Yet, within core samples are statistically similar and we attribute their deposition to a single event with slightly variable initial activities. LWD-7.45 is also interpreted as a single event due to the lack of a significant decrease in activity with depth, although it is possible that

Figure 5. (a) Unit stream power ($\omega = \gamma QS/w$) [cf. *Magilligan*, 1992] along the Ducktrap River, where γ is the specific weight of water (9810 N m^{-3}), Q is bankfull discharge in m^3 s^{-1}, S is slope, and w is the channel width (m) calculated from regional curves in the work by *Magilligan et al.* [2008a]. Field delineation of two different transport regimes is further validated by this simple calculation of energy expended on the channel bed at bankfull discharge. (b) The Ducktrap River profile along the study reach showing site locations and field observations of sediment/transport regimes. Dashed lines denote tributary sites. (c) Locations and activities of thalwegs and emergent bar (0–5 cm) samples along the study reach with the mean (5.12 mBq m^{-2}) and 1 σ above (7.72 mBq m^{-2}) and below (2.52 mBq m^{-2}), denoted by horizontal lines. These values are used as proxies to constrain the range of initial sediment activities for calculating sediment storage times. Arrows indicate inferred trends in activities with distance from the mouth. Note the steady decline in surface activities of ~2.8 mBq m^{-2} km^{-1} from Tucker Brook (TB) to Black Brook (BB) (gray box) indicating overall a greater rate of decay (particle submersion) compared to exposure (fallout dosing) in this reach. Solid symbols denote tributary samples.

Table 3. The ^{7}Be Activities and Sediment Surface Area Data for Ducktrap River Samples[a]

Sample Location	Sample Depth (cm)	SSA (m^2 kg^{-1})	^{7}Be (mBq kg^{-1})	^{7}Be/SSA (mBq m^{-2})	Analytical Error (%)
			22 July 2006[b]		
T-11.6	surface	2,160	11,900	5.51	7.0
TB-LWD	0–5	1,740	2,900	1.70	9.7
TB-LWD	5–10	1,610	2,400	1.49	8.5
TB-LWD	10–15	1,860	2,000	1.09	10.1
TB-LWD	15–20	1,920	1600	0.85	10.6
TB-LWD	20–25	1,680	ND	ND	ND
TB-EB	0–5	1,640	3,000	1.81	9.7
TB-EB	5–10	1,850	2,200	1.17	10.0
TB-EB	10–15	1,660	ND	ND	ND
TB-EB	15–20	1,770	ND	ND	ND
LWD-10.7	0–5	2,100	4,500	2.16	7.0
LWD-10.7	5–10	1,750	4,100	2.33	9.5
LWD-10.7	10–15	1,740	5,500	3.14	10.1
EB-10.7	0–5	1,470	11,600	7.86	8.4
EB-10.7	5–10	1,490	ND	ND	ND
EB-10.7	10–15	1,550	ND	ND	ND
EB-10.7	15–20	1,340	ND	ND	ND
			2 August 2006[b]		
T-9.1	surface	1,260	13,400	10.62	7.2
B-9.1	0–5	1,610	5,200	3.22	9.8
B-9.1	5–10	1,560	4,700	2.98	10.1
B-9.1	10–15	1,410	ND	ND	ND
B-9.1	15–20	1,500	ND	ND	ND
B-9.1	20–25	1,440	ND	ND	ND
T-8.8	surface	1,360	11,600	8.51	6.3
EB-8.8	0–5	1,390	7,600	5.50	7.5
EB-8.8	5–10	1,770	ND	ND	ND
EB-8.8	10–15	1,620	ND	ND	ND
EB-8.8	15–20	1,620	ND	ND	ND
EB-8.8	20–25	1,330	ND	ND	ND
T-8.4	surface	1,610	6,200	3.85	8.7
LWD-8.4	0–5	1,560	9,300	5.95	6.4
LWD-8.4	5–10	1,490	9,900	6.68	7.0
LWD-8.4	10–15	1,520	10,800	7.09	5.7
			3 August 2006[b]		
T-7.9	surface	1,520	8,800	5.78	8.1
B-7.9	0–5	1,540	8,500	5.51	9.3
B-7.9	5–10	1,610	8,200	5.06	6.6
B-7.9	10–15	1,340	5,200	3.85	8.2
T-7.5	surface	1,380	7,300	5.28	8.5
LWD-7.5	0–5	1,750	11,800	6.71	5.8
LWD-7.5	5–10	1,680	4,000	2.40	9.1
LWD-7.5	10–15	2,000	4,000	2.00	9.1
LWD-7.5	15–20	1,920	ND	ND	ND
LWD-7.5	20–25	1,830	ND	ND	ND
EB-7.5	0–5	1,360	5,400	3.93	9.5
EB-7.5	5–10	1,440	8,600	6.11	9.5
EB-7.5	10–15	1,830	4,100	2.23	12.3
EB-7.5	15–20	1,550	1,800	1.19	15.4
EB-7.5	20–25	1,770	ND	ND	ND
EB-7.5	25–30	1,800	ND	ND	ND
EB-7.5	30–35	1,670	ND	ND	ND
EB-7.5	35–40	1,810	ND	ND	ND
LWD-7.45	0–5	1,650	5,700	3.48	9.3
LWD-7.45	5–10	1,640	4,400	2.68	10.9
LWD-7.45	10–15	1,600	4,200	2.63	9.1
LWD-7.45	15–20	1,510	4,000	2.66	8.2
LWD-7.4	0–5	1,660	9,000	5.41	7.8
LWD-7.4	5–10	1,850	4,700	2.57	9.2
LWD-7.4	10–15	1,710	5,000	2.90	6.7
LWD-7.4	15–20	1,690	2,000	1.16	12.2
LWD-7.4	20–25	1,540	ND	ND	ND
LWD-7.4	25–30	1,580	ND	ND	ND
			14 August 2006[b]		
T-7.2	surface	1,650	5,400	3.25	11.0
LWD-7.2	0–5	1,460	ND	ND	ND
LWD-7.2	5–10	1,610	ND	ND	ND
LWD-7.2	10–15	1,350	ND	ND	ND
LWD-7.2	15–20	1,370	ND	ND	ND
LWD-7.2	20–25	1,390	ND	ND	ND
LWD-7.2	25–30	1,240	ND	ND	ND

Table 3. (continued)

Sample Location	Sample Depth (cm)	SSA (m^2 kg^{-1})	^{7}Be (mBq kg^{-1})	^{7}Be/SSA (mBq m^{-2})	Analytical Error (%)
EB-7.2	0–5	1,540	4,800	3.12	13.2
EB-7.2	5–10	1,430	ND	ND	ND
EB-7.2	10–15	1,200	ND	ND	ND
EB-7.2	15–20	1,500	ND	ND	ND
EB-7.2	20–25	1,470	ND	ND	ND
EB-7.2	25–30	1,300	ND	ND	ND
T-6.9	surface	1,140	5,800	5.11	9.8
B-6.9	0–5	1,540	7,500	4.88	8.1
B-6.9	5–10	1,210	4,200	3.47	9.8
B-6.9	10–15	1,270	4,500	3.58	9.5
B-6.9	15–20	1,290	3,800	2.90	8.9
			15 August 2006[b]		
T-6.0	surface	940	ND	ND	ND
LWD-6.0	0–5	1,160	3,600	3.09	13.7
LWD-6.0	5–10	1,170	2,400	2.05	14.6
LWD-6.0	10–15	1,040	7,200	6.95	8.6
LWD-6.0	15–20	1,270	ND	ND	ND
LWD-6.0	20–25	1,080	ND	ND	ND
LWD-6.0	25–30	1,050	ND	ND	ND
LWD-6.0	30–35	1,210	ND	ND	ND
LWD-6.0	35–40	1,100	ND	ND	ND
EB-6.0	0–5	970	ND	ND	ND
EB-6.0	5–10	1,390	ND	ND	ND
EB-6.0	10–15	1,130	ND	ND	ND
EB-6.0	15–20	740	ND	ND	ND
EB-6.0	20–25	680	ND	ND	ND
BB-T	surface	2,680	13,500	5.05	8.6
T-5.3	surface	1,120	8,100	7.26	9.2
B-5.3	0–5	950	ND	ND	ND
B-5.3	5–10	1,000	ND	ND	ND
B-5.3	10–15	830	ND	ND	ND
B-5.3	15–20	840	ND	ND	ND
			16 August 2006[b]		
T-5.1	surface	1,060	7,200	6.82	11.5
LWD-5.1	0–5	800	ND	ND	ND
LWD-5.1	5–10	890	ND	ND	ND
LWD-5.1	10–15	720	ND	ND	ND
LWD-5.1	15–20	730	ND	ND	ND
LWD-5.1	20–25	800	ND	ND	ND
LWD-5.1	25–30	710	ND	ND	ND
EB-5.1	0–5	880	4,400	4.98	12.7
EB-5.1	5–10	940	ND	ND	ND
KB-T	surface	3,060	18,100	5.91	6.7
T-3.0	surface	900	6,600	7.34	11.3

[a]Bold sample locations indicate tributary samples. SSA, sediment surface area; ND, not detectable.
[b]Dates collected.

the 0–5 cm sample represents an additional event. These three bars (LWD-10.7, LWD-8.4, and LWD-7.45) are all calculated to be new (top sample) to a maximum of 82 days old (LWD-7.45 bottom) and we interpret their deposition as arising from full scouring of the previous sediment bar during the rising limb of the hydrograph followed by deposition on the falling limb. This finding suggests that complete bar renewal occurs with each significant discharge event (Figure 7 and Table 4).

[18] The second profile type documented in the submerged sediment cores is characterized by multidepositional events with systematic declines in sample activities with core depth (Figure 7). This activity pattern pertains to profiles B-9.1, B-7.9, LWD-7.5, LWD-7.4, B-6.9, and LWD-6.0 (Figures 7, 8, and 9). In each of these cores there is a decrease in activity with depth below the sediment surface. LWD-7.5 and LWD-7.4 both display activity decreases from surface values of approximately 6 mBq m^{-2} to non-detectable ^{7}Be in the basal samples indicating multiple depositional and/or scour events (~"new" depositional ages in the 0–5 cm samples to >210 days in the basal samples) (Tables 3 and 4). Likewise, LWD-6.0 is characterized by a systematic decrease in activity with depth but with a much lower surface sample (0–5 cm) activity (3.09 mBq m^{-2}) (due to longitudinal thalweg activity decay (see Figure 5)) as well as an anomalously high 10–15 cm sample activity that may result from a localized perturbation (slumping, rilling, etc.). B-9.1 has a similar profile to LWD-7.5 and LWD-7.4, but appears to record only one recent depositional event on top of older event(s) that are now devoid of ^{7}Be activity (Figure 9). B-7.9 and B-6.9 both display similar profiles indicating multiple depositional events and contain ^{7}Be throughout the bar, indicating complete bar mobilization during notable discharge events followed by multistage bar construction (Figure 7). Sediment storage times for B-7.9 and B-6.9 are constrained to less than 26 and 35 days old at

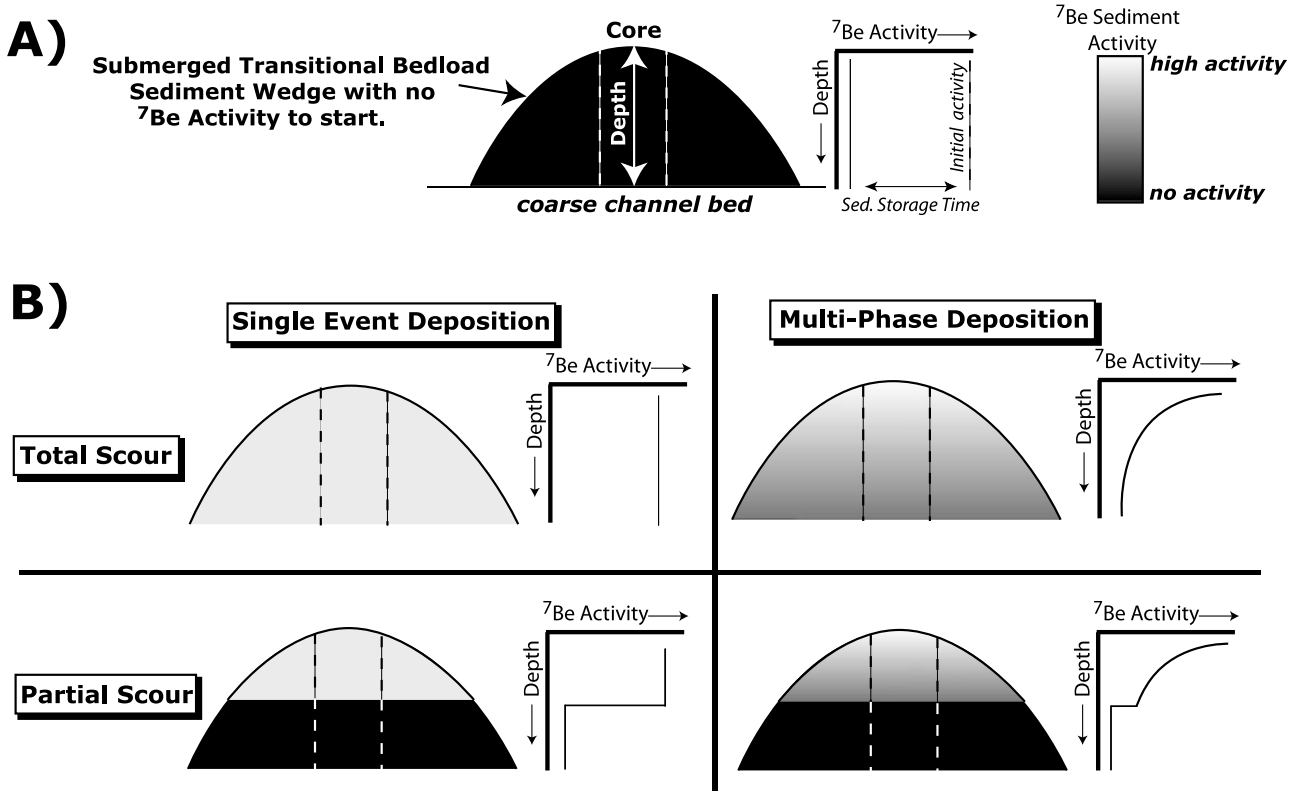

Figure 7. Conceptual model of scour/deposition histories for in-channel sediment bars and associated ^{7}Be activity profiles with depth down the core. (a) Initial sediment bar with no activity and associated activity profile (solid line). The dashed line on the activity versus depth plot indicates initial activity of incoming sediment with the difference in this value with the observed profile yielding storage time through equation (1). (b) Matrix of scour and deposition events with associated activity profiles. Color gradient indicates relative activity of sediment and sediment storage age (white, new and high activity; black, old and no activity). Bar shape is idealized and not representative of the wide-ranging shapes observed in the field.

the top to 54 and 75 days old at the bottom samples, respectively, using the CIA methodology (Table 4).

[19] The third profile type observed is characterized by the lack of detectable ^{7}Be activity throughout the bar, as with LWD-7.2, B-5.3, and LWD-5.1. In these profiles no ^{7}Be is detected in the profile and only three rational explanations exist: (1) the bars have been isolated from deposition for a greater amount of time than can be detected using the established methodology (~106 to 210 days depending on the initial activity used); (2) the bars are experiencing periods of deposition and/or scour but the sediment being deposited lacks activity (due to reach averaged decay shown in Figure 5); or (3), the top layers that would have ^{7}Be activity have been recently scoured and no subsequent transitional bed load deposition has occurred. While these options are clearly simplified and other localized phenomena cannot be ruled out, we choose the latter explanation based on the presence of ^{7}Be activity in adjacent thalweg and emergent bar samples, which indicates that sediment with ^{7}Be activity is available for deposition under proper hydraulic conditions. It is likely that these bars act as sites of longer-term sediment storage and that the sampling time happened to coincide with a period of recent scour, leading to a lack of detectable ^{7}Be even in the surface samples.

5.3. Emergent Bar Activities and Storage Times

[20] Emergent bars were sampled and cored at river kilometers 10.7, 8.8, 7.5, 7.2, 6.0, and 5.1 and at Tucker Brook adjacent to TB-LWD (Figures 1 and 10). Overall, profiles show little ^{7}Be activity below the 0–5 cm sample indicating these emergent bars are sites of long-term accumulation and store the majority of their sediment for timescales greater than the detection limit of ^{7}Be (>210 days). The activity in the 0–5 cm sample can be attributed to a combination of inherited ^{7}Be and subsequent exposure and in growth of ^{7}Be from atmospheric fallout, which even in reference soils rarely reaches 5 cm of depth penetration [*Kaste et al.*, 2002]. Exceptions are TB-EB, EB-7.5, and EB-6.0. TB-EB, taken adjacent to TB-LWD, displays activity down to 10 cm indicating that the top 10 cm has recently been deposited (potentially coeval with TB-LWD based on similar activities) with little atmospheric in growth, while EB-6.0 is devoid of activity throughout the profile indicating very recent scour of the meteoric cap and/or deposition of dead sediment (Figure 10). EB-7.5 is anomalous in that it has detectable activity down to 20 cm and (besides the 0–5 cm sample) shows a decrease in activity coincident with an increase in depth. This is attributed to the

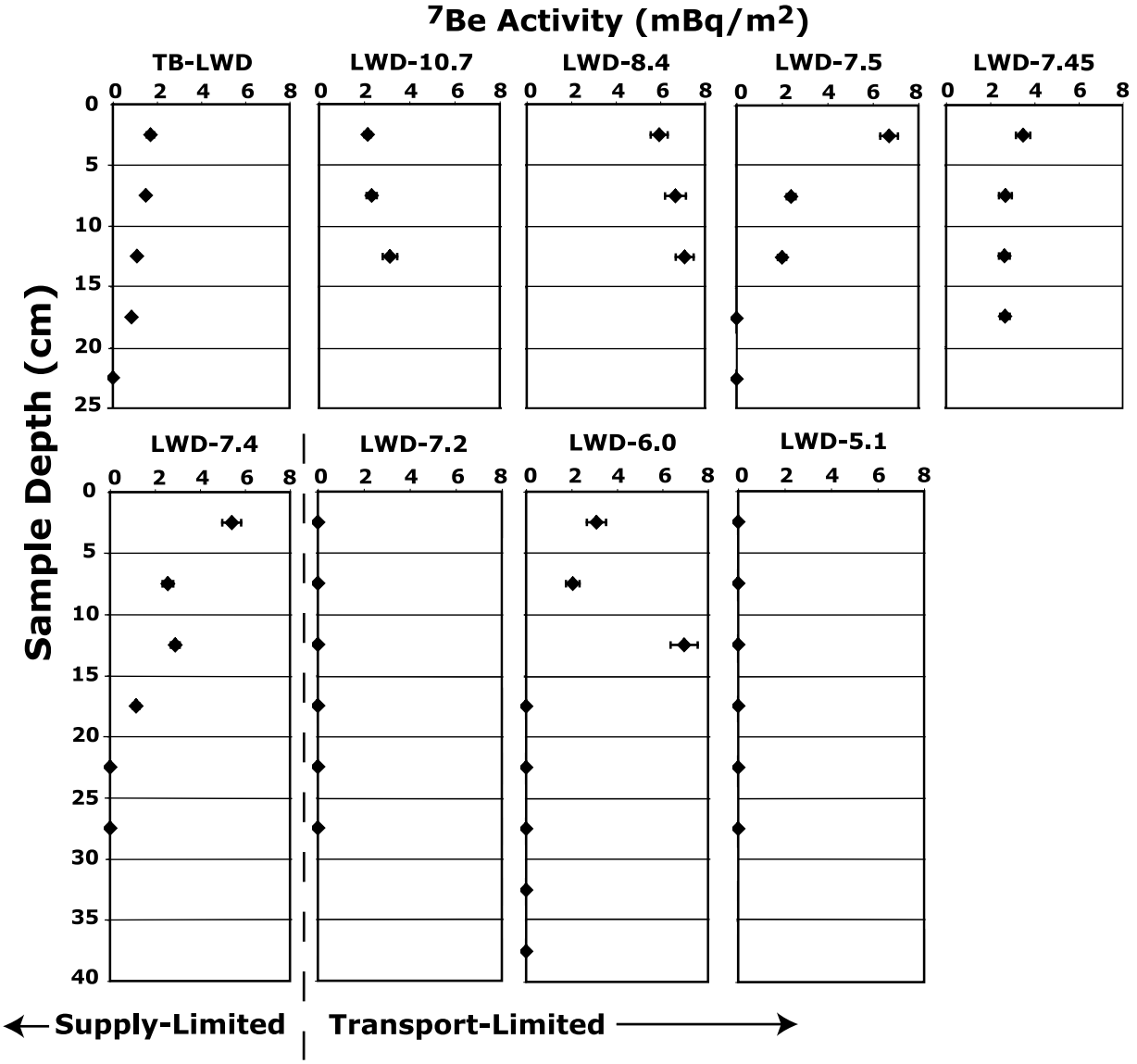

Figure 8. The ^{7}Be activity (mBq m^{-2}) versus sample depth for submerged sediment bars associated with LWD. All bars were sampled entirely down to the interface with the coarser channel bed (gravel to cobble sized particles).

deposition of sediment with decreased activity and/or the lack of exposure time of the 0–5 cm sample to atmospheric fallout, with the latter indicating that it was recently deposited. While storage time estimates using the CIA methodology are complicated on emergent bars when exposure histories are unknown, the presence of leaf litters can act as a proxy for depositional age. We assume that all leaf litters are deposited in the late fall when higher recurrence interval storms and defoliation of the trees coincide to create such deposits. In the example of EB-7.5 this would indicate that sediment has been stored for close to 2 years at the bottom of the profile and approximately 1 year in EB-8.8 and EB-6.0 (Figure 10).

5.4. Calculated Sediment Accumulation Rates

[21] Accumulation rates for several activity profiles (TB-LWD, LWD-7.5, LWD-7.4, EB-7.5, and B-6.9) were calculated where ^{7}Be data were sufficient (minimum of three points with detectable activity) and exponential decay trends were observed (Figure 11). Rates of mass flux to the depositional bars were determined through the following rearrangement of the basic CIA model (equation (1)) whereby mass is substituted for time [*Appleby and Oldfield*, 1992]:

$$A = A_0\, e^{-\lambda m/r} \tag{2}$$

where m is the cumulative dry mass per unit area above the layer (g cm^{-2}) and r is the mass flux (g cm^{-2} d^{-1}). This model assumes a constant initial activity where the rate of accumulation of ^{7}Be activity is proportional to the mass accumulation and, therefore, activity must decline monotonically with depth [*Appleby and Oldfield*, 1992]. Analysis of five profiles indicates varying accumulation rates over the

Table 4. Calculated Storage Times for Submerged Sediment Bars Using the Mean and 1 σ Above and Below CIA Values[a]

	CIA Storage Times (days)		
	2.52 mBq m^{-2} (SSA)	5.12 mBq m^{-2} (SSA)	7.72 mBq m^{-2} (SSA)
LWD			
TB-LWD	30 to >106	85 to >160	116 to >210
LWD-10.7	new	~55	~82
LWD-8.4	new	New	~13
LWD-7.5	new to >106	new to >160	11 to >210
LWD-7.45	new	30 to 50	61 to 82
LWD-7.4	new to >106	new to >160	27 to >210
LWD-7.2	>106	>160	>210
LWD-6.0	new to >106	39 to >160	70 to >210
LWD-5.1	>106	>160	>210
Boulder			
B-9.1	new to >106	36 to >160	67 to >210
B-7.9	new	new to 22	26 to 54
B-6.9	new	4 to 44	35 to 75
B-5.3	>106	>160	>210

[a]See Figure 5c for mean and 1σ above and below CIA values. Storage times are constrained using the top and bottom samples in each bar and reported as top sample storage time to bottom sample storage time. CIA, constant initial activity. "New" indicates recent sediment deposition evidenced by negligible ^{7}Be decay from the initial activity.

applicable ^{7}Be time period (<210 days): profiles in the supply-limited section have the lowest accumulation rates (0.2 g cm^{-2}), with significantly higher accumulation rates for the Tucker Brook (TB-LWD) and B-6.9 (transport-limited section) profiles (0.4 and 0.7 g cm^{-2}, respectively) (Figure 11). There appears to be no significant difference between EB-7.5 and the adjacent submerged bars (LWD-7.5 and LWD-7.4); however, the 0–5 cm sample had to be adjusted to 7.72 mBq m^{-2} (the highest constant initial activity) in EB-7.5 due to the anomalously low activity value analyzed. We believe that this interpretation is justified as we see very few samples with activities higher than 7.72 mBq m^{-2} and the activity profile displays a clear exponential decline, with atmospheric inputs only affecting the surface sample (0–5cm depth). In general, the high R^2 values, the consistent agreement of predicted initial activities with the CIA model range (excluding EB-7.5), and the agreement between accumulation rates and the two different transport regimes, provide further justification for the use of the CIA methodology and provide rough estimates of in-channel sediment deposition rates over short timescales (~100 days) associated with channel obstructions. We caution, however, that these rates are not indicative of overall bed aggradation/erosion, cannot be applied rigorously toward a sediment budget estimate [*Dietrich et al.*, 1982], and merely represent an estimate of short-term sediment bar accumulation rates as constrained by the CIA method.

6. Discussion

6.1. Sediment Storage Times: Controls, Variability, and Implications

[22] Considerable work has documented the hydrological and ecological role that in-channel obstructions play in

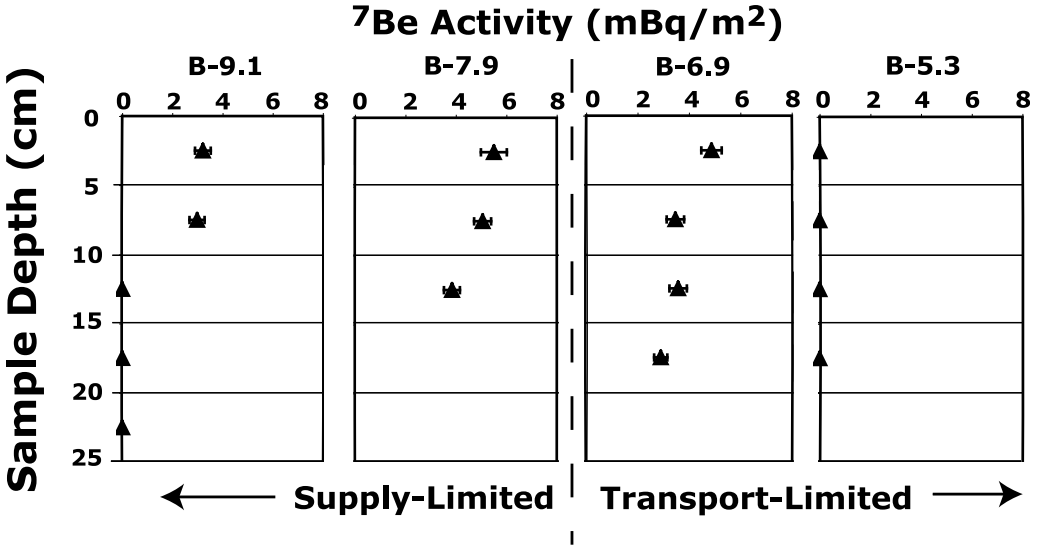

Figure 9. The ^{7}Be activity (mBq m^{-2}) versus sample depth for submerged sediment bars associated with boulders. All bars were sampled entirely down to the interface with the coarser channel bed (gravel to cobble sized particles).

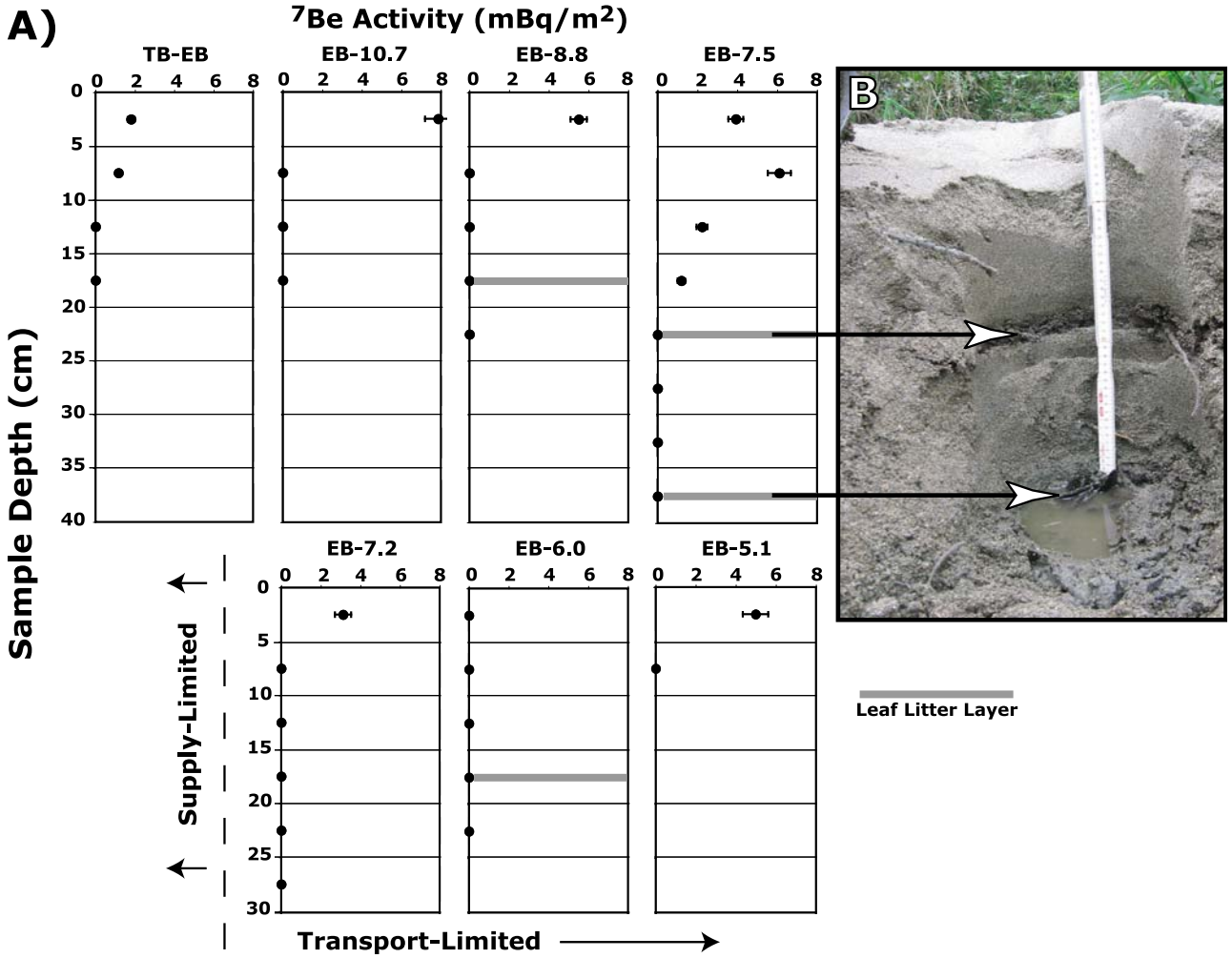

Figure 10. (a) The ^{7}Be activity (mBq m^{-2}) versus sample depth for emerged sediment bars. The presence of leaf litters in the activity profiles are denoted by gray lines and are interpreted to represent late fall depositional events. (b) Two leaf litters (arrows) observed in the EB-7.5 profile indicating two fall seasons of deposition. All emergent bars were sampled down to the water level.

creating both hydraulic and substrate heterogeneity within streams of all sizes. Likewise, several studies have attempted to quantify particle transit times in various watersheds using stochastic models and parameterization [*Malmon et al.*, 2003], while studies of fine-particle residence times associated with pools has documented short storage times ($\ll$1 year) and mobility at discharges equal to half-bankfull using scour chains [*Lisle and Hilton*, 1999]. However, no studies to our knowledge have attempted to quantify transitional bed load storage times associated with in-channel obstructions despite the proven importance of sediment sequestration by such features. Such storage times have implications for understanding watershed-scale transport rates [*Syvitski et al.*, 2005], nutrient retention [*Bilby*, 1981], sediment budgets [*Dietrich et al.*, 1982], and both natural and restored fluvial and riparian ecosystem dynamics [*Montgomery et al.*, 2003].

[23] Results using the CIA methodology and field observations indicate two dominant transport regimes along the Ducktrap River characterized by differing storage times (Figure 12), unit stream power values (Figure 5), and accumulation rates (Figure 11). Steeper gradients in the supply-limited reach produce greater stream power values capable of mobilizing fine-grained sediment bars associated with channel obstructions with great frequency (generally < 100 day sediment storage times) during relatively low magnitude discharge events (~70% of the 2 year recurrence interval (see Figure 12)). In contrast, the transport-limited reach is characterized by much greater sediment storage times associated with channel obstructions (in most cases greater than the detection limit of ~210 days) due to lower unit stream power (about one fourth of the supply-limited reach average) as well as greater overall wood frequency (Figure 3). Wood $\geq$20 cm in diameter along the transport-limited reach is nearly twice as frequent (110 pieces per kilometer) as in the supply-limited reach (56 pieces per kilometer), causing increased hydraulic resistance and diminished erosive power for a given discharge [*Manga and Kirchner*, 2000]. This increased channel roughness when coupled with already diminished slope-based proxies of

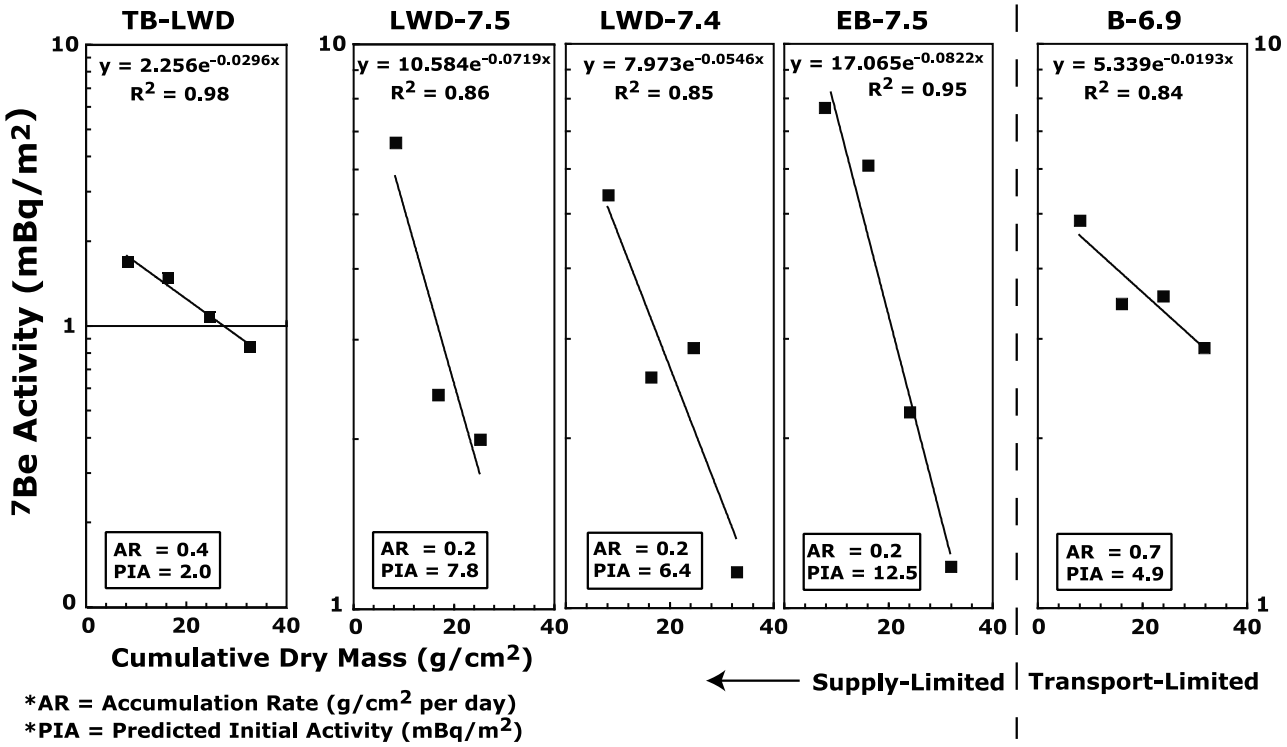

Figure 11. The ^{7}Be activity (mBq m^{-2}) plotted against cumulative dry mass (g cm^{-2}) on a lognormal scale in five of the best behaved cores with associated exponential regression equations and R^2 values. The y intercept is the calculated initial activity at deposition based on the exponential line of best fit, while the slope of the line (equal to $-\lambda/r$ from equation (2)) is used to determine approximate accumulation rates (AR) for each profile. Predicted initial activities are calculated using the exponential line of best fit for each profile and accounting for the intercept with the mass of half of the top sample bin for each profile (i.e., consistent with 2.5 cm core depth). Note different y axis scale for TB-LWD.

erosion potential (unit stream power) limits the frequency with which bars in the transport-limited reach undergo total mobilization, a finding consistent with the abundant profiles lacking any or only partial ^{7}Be throughout the reach (Figure 12).

[24] Variability is not only evident between different transport regimes using the CIA technique, but also among channel obstruction type. The current LWD literature remains unresolved about which techniques and materials are best for restoring ecological, hydrologic, and geomorphic diversity and function in disturbed streams [*Montgomery*, 1997]. Both boulders and LWD have been used extensively in restoration efforts across the country with one of the main focuses being placed on the ability of such additions to regulate sediment and nutrient flux to enhance stream ecosystems [*Bilby and Likens*, 1980]. Previous studies have documented considerable discrepancies in sediment storage volumes between boulders and LWD in the Pacific Northwest, where in-channel LWD stored approximately 5 times more sediment than in-channel boulders in both tributaries and main stem streams [*May and Gresswell*, 2003]. In the Ducktrap River boulder deposits tend to be slightly less voluminous (as well as shallower) and less abundant (regardless of transport regime only four were found to be suitable for coring) than those of LWD. Boulder bars also appear to be frequently scoured and mobilized down to the coarse channel bed, whereas bars associated with LWD show greater diversity in mobilization histories, potentially attesting to the greater hydraulic complexity created by logs and debris jams [*Manners et al.*, 2007].

[25] While wood size and frequency has been diminished by twentieth century logging practices in the Ducktrap watershed [*Magilligan et al.*, 2008a], it is expected that with maturing riparian forests will come increased in-channel wood size, and as a result, increased sediment storage times and volumes associated with LWD. This in turn promotes habitat heterogeneity [*Yarnell et al.*, 2006], reduces embeddedness of spawning gravels, and promotes a host of other positive results with respect to ecosystem function. These positive attributes of LWD when coupled with the relative dearth of sediment storage by boulders, the viability of sourcing LWD throughout forested streams by tree senescence from riparian zones, and the proven ability to provide sediment storage at greater temporal and spatial scales (as shown by this study) argues for greater restoration efficacy by LWD than boulders, especially once riparian forest age structures and size are restored to prehistoric levels in anthropogenically disturbed watersheds like the Ducktrap River.

6.2. The ^{7}Be Technique Potential and Caveats

[26] In this study we have documented the validity of using cosmogenic ^{7}Be decay systematics coupled with a

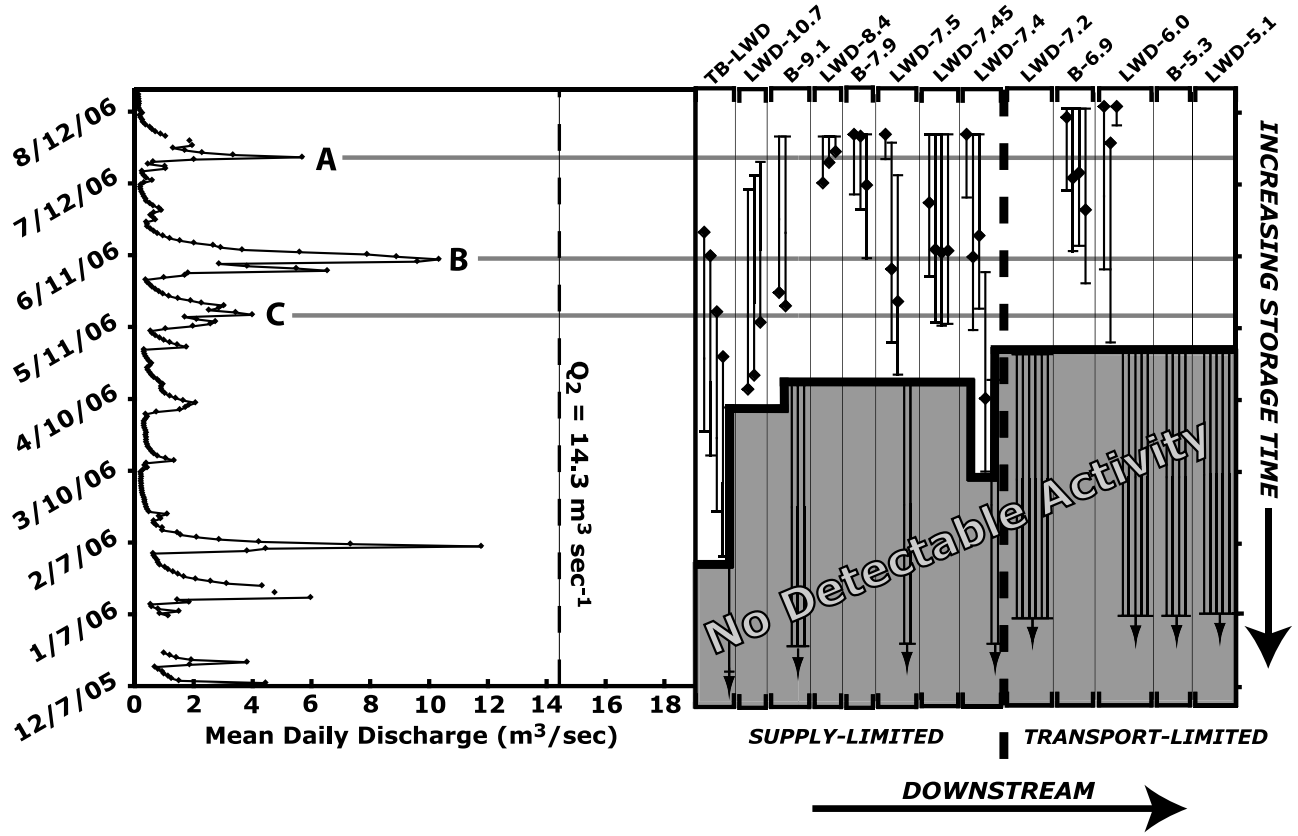

Figure 12. Plot of the calculated deposition time range based on the CIA model for each submerged bar depth profile sample along with hydrograph data. Diamonds represent the optimal time of deposition based on the constant initial activity (7.72, 5.12, or 2.52 mBq m^{-2}) that best matched the adjacent thalweg and emergent bar surface samples as shown in Figure 5c. Sampled bars are in order from farthest upstream to most downstream. Samples falling below the thick black line indicate samples with no detectable ^{7}Be and ages greater than the sensitivity of the CIA methodology. Horizontal lines linking the hydrograph and depositional times of the samples denote discharge events (lines a, b, and c) potentially responsible for the deposition of samples with detectable activities. In contrast, little can be said about the timing and magnitude of flows responsible for the transport/deposition of samples lacking detectable ^{7}Be. The Q_2 vertical on the hydrograph represents the recurring 2 year bankfull discharge. Note the *y* axis is the same for both the hydrograph and the calculated sediment deposition times.

CIA sediment aging model to constrain transitional bed load storage times. However, certain precautions must be taken to properly implement this methodology in future studies. Because of the short half-life associated with ^{7}Be (~53 days), this technique is best utilized in lower-order streams where long-term in-channel sediment storage is less pervasive and where sediment inputs can be well constrained. Significant problems with the technique may arise if significant fine-grained sediment storage occurs subaqueously on channel bottoms. Specifically, longer-term in-channel residence times (greater decay) coupled with proportionally less exposed sediment on channel margin bars may lead to an activity dilution effect. This will lead to diminished or dead initial activities and will render the observed timescales of the technique inadequate for constraining storage times of any utility. The CIA technique depends on having a large portion of the sediment stored outside of the low-flow channel where it is available for atmospheric exposure and redosing by ^{7}Be. Due to this constraint the technique is best applied in higher-gradient step-pool systems more consistent with the supply-limited reach discussed in this study. Other potential complicating factors include (1) frequent landsliding or bank collapse events, which may overwhelm a system with dead sediment and go undetected without extensive field reconnaissance; (2) periodic exposure of submerged bars (in low-flow conditions) to atmospheric fallout, which will overprint the inherited signal and greatly complicate interpretations and the utility of the technique; and (3) seasonal variations, where sediments sampled directly after winter may be devoid of activity simply due to decreased winter fallout and/or coverage of exposed sediments by snow and ice and not related to submerged storage times (the principle reason we sampled in August). Last, in systems where initial activities are difficult to constrain and the CIA methodology lacks application, the simple presence/absence of ^{7}Be (presence indicates <210 days of inundation) can provide ample information about the relative timing of deposition and mobiliza-

tion events and may provide greater spatial and temporal resolution than previous techniques (scour chains, etc.) where constant monitoring and equipment upkeep may be too laborious.

7. Conclusions

[27] Short-term sequestration of fine-grained sediment over the period of months to less than 1 year by in-channel LWD and boulders has been documented using a novel application of cosmogenic ^{7}Be coupled to a CIA sediment storage aging model. In addition, stratigraphic evidence provided by buried leaf litters in emerged channel margin sediment bars suggests that they are sites of longer-term storage and aggradation on the order of a year to several years. Reach-scale variability in unit stream power calculations and LWD frequency affect sediment storage times, with transport-limited reaches providing longer-term (>100 days) sediment sequestration associated with in-channel obstructions than supply-limited ones (<100 days). Furthermore, greater in-channel transitional bed load sediment storage times and volumes, greater spatial frequency of sediment sequestration, and naturally viable LWD sourcing mechanisms argue for greater LWD efficacy in channel restoration projects than boulders. This finding is underscored in the Ducktrap River by diminished wood frequency and size related to twentieth century logging [*Magilligan et al.*, 2008a], and it is expected that as riparian forests mature that in-channel sediment storage times, volumes, and bar frequency associated with LWD will increase, providing even greater ecogeomorphic benefits.

[28] Future studies should expand on the work presented here by applying this technique to other channel features (check dams, old growth LWD, pool storage, etc.) with the ultimate goal of being able to quantitatively build watershed sediment budgets and model sediment particle trajectories with improved confidence and precision [*Dietrich et al.*, 1982]. Such future applications will be beneficial to a host of disciplines from environmental restoration to aquatic nutrient cycling, and should illuminate key relationships between sediment dynamics, channel morphology, and anthropogenic disturbances in forested watersheds. In this study we have utilized a novel application of the fallout radionuclide ^{7}Be to better understand storage times associated with channel obstructions in an anthropogenically disturbed watershed, and when properly applied, we contend ^{7}Be provides an invaluable tool for deciphering the complex interactions between sediment dynamics and channel components and form at short temporal scales.

[29] **Acknowledgments.** This research was generously funded by a Geological Society of America Graduate Student Research Grant (8253-06), a National Fish and Wildlife Foundation grant (2004-0010-022), and National Science Foundation grants (BCS-0724348 and EAR-0650533). We would like to thank the U.S. Fish and Wildlife Service Gulf of Maine Coastal Program and the Department of Marine Resources, Bureau of Sea Run Fisheries (formerly the Maine Atlantic Salmon Commission), for assistance with site location and selection; C. E. Renshaw for helpful discussions; and Sara Gilbert and Abigail Kennedy for field and laboratory assistance. Careful reviews by Stephen Lancaster, Peter Whiting, Jose Constantine, and two anonymous reviewers greatly improved previous versions of this manuscript.

References

Aalto, R., L. Maurice-Bourgoin, T. Dunne, D. R. Montgomery, C. A. Nittrouer, and J.-L. Guyot (2003), Episodic sediment accumulation on Amazonian flood plains influenced by El Niño/Southern Oscillation, *Nature*, *425*, 493–497, doi:10.1038/nature02002.

Appleby, P. G., and F. Oldfield (1992), Application of lead-210 to sedimentation studies, in *Uranium-Series Disequilibrium*, edited by M. Ivanovich and R. S. Harmon, pp. 731–778, Oxford Univ. Press, New York.

Bilby, R. E. (1981), Role of organic debris dams in regulating the export of dissolved and particulate matter from a forested watershed, *Ecology*, *62*, 1234–1243, doi:10.2307/1937288.

Bilby, R. E., and G. E. Likens (1980), Importance of organic debris dams in the structure and function of stream ecosystems, *Ecology*, *61*, 1107–1113, doi:10.2307/1936830.

Blake, W. H., D. E. Walling, and Q. He (2002), Using cosmogenic beryllium-7 as a tracer in sediment budget investigations, *Geogr. Ann., Ser. A*, *84*, 89–102.

Bonniwell, E. C., G. Matisoff, and P. J. Whiting (1999), Determining the times and distances of particle transit in a mountain stream using fallout radionuclides, *Geomorphology*, *27*, 75–92, doi:10.1016/S0169-555X(98)00091-9.

Brunauer, S., P. H. Emmett, and E. Teller (1938), Adsorption of gases in multimolecular layers, *J. Am. Chem. Soc.*, *60*, 309–319, doi:10.1021/ja01269a023.

Daniels, M. D., and B. L. Rhoads (2004), Effect of large woody debris configuration on three-dimensional flow structure in two low-energy meander bends at varying stages, *Water Resour. Res.*, *40*, W11302, doi:10.1029/2004WR003181.

Dietrich, W. E., T. Dunne, N. F. Humphrey, and L. M. Reid (1982), Construction of sediment budgets for drainage basins, in *Sediment Budgets and Routing in Forested Drainage Basins*, edited by F. J. Swanson et al., *Gen. Tech. Rep. PNW-141*, pp. 5–23, U.S. Dep. of Agric. For. Serv., Corvallis, Oreg.

Dosseto, A., S. P. Turner, and G. B. Douglas (2006), Uranium-series isotopes in colloids and suspended sediments: Timescales for sediment production and transport in the Murray-Darling River system, *Earth Planet. Sci. Lett.*, *246*, 418–431, doi:10.1016/j.epsl.2006.04.019.

Feng, H., J. K. Cochran, and D. J. Hirschberg (1999), ^{234}Th and ^{7}Be as tracers for the transport and dynamics of suspended particles in a partially mixed estuary, *Geochim. Cosmochim. Acta*, *63*, 2487–2505, doi:10.1016/S0016-7037(99)00060-5.

Fitzgerald, S. A., J. Val Klump, P. W. Swarzenski, R. A. Mackenzie, and K. D. Richards (2001), Beryllium-7 as a tracer of short-term sediment deposition and resuspension in the Fox River, Wisconsin, *Environ. Sci. Technol.*, *35*, 300–305, doi:10.1021/es000951c.

Gregg, S. J., and K. S. W. Sing (Eds.) (1982), *Adsorption, Surface Area and Porosity*, 2nd ed., 303 pp., Academic, London.

Hawley, N., J. A. Robbins, and B. J. Eadie (1986), The partitioning of ^{7}beryllium in fresh water, *Geochim. Cosmochim. Acta*, *50*, 1127–1131, doi:10.1016/0016-7037(86)90393-5.

He, Q., and D. E. Walling (1996a), Interpreting particle size effects in the adsorption of ^{137}Cs and unsupported ^{210}Pb by mineral soils and sediments, *J. Environ. Radioact.*, *30*, 117–137, doi:10.1016/0265-931X(96)89275-7.

Kaste, J. M., S. A. Norton, and C. T. Hess (2002), Environmental chemistry of beryllium-7, *Rev. Mineral. Geochem.*, *50*, 271–289.

Kaste, J. M., A. M. Heimsath, and B. C. Bostick (2007), Short-term soil mixing quantified with fallout radionuclides, *Geology*, *35*, 243–246, doi:10.1130/G23355A.1.

Keller, E. A., and F. J. Swanson (1979), Effects of large organic material on channel form and fluvial processes, *Earth Surf. Processes*, *4*, 361–380, doi:10.1002/esp.3290040406.

Keller, E. A., A. MacDonald, T. Tally, and N. J. Merritt (1995), Effects of large organic debris on channel morphology and sediment storage in selected tributaries of Redwood Creek, *U.S. Geol. Surv. Prof. Pap.*, *1454-P*.

Lal, D., P. K. Malhotra, and B. Peters (1958), On the production of radioisotopes in the atmosphere by cosmic radiation and their application to meteorology, *J. Atmos. Terr. Phys.*, *12*, 306–328, doi:10.1016/0021-9169(58)90062-X.

Lancaster, S. T., S. K. Hayes, and G. E. Grant (2001), Modeling sediment and wood storage and dynamics in small mountainous watersheds, in *Geomorphic Processes and Riverine Habitat*, *Water Sci. Appl.*, vol. 4, edited by J. M. Dorava et al., pp. 85–102, AGU, Washington, D.C.

Lisle, T. (1979), A sorting mechanism for a riffle-pool sequence: Summary, *Geol. Soc. Am. Bull.*, *90*, 616–617, doi:10.1130/0016-7606(1979)90<616:ASMFAR>2.0.CO;2.

Lisle, T. E. (1986), Stabilization of a gravel channel by large streamside obstructions and bedrock bends, Jacoby Creek, northwestern California, *Geol. Soc. Am. Bull.*, *97*, 999–1011.

Lisle, T. E., and S. Hilton (1999), Fine bed material in pools of natural gravel bed channels, *Water Resour. Res.*, *35*, 1291–1304, doi:10.1029/1998WR900088.

Magilligan, F. J. (1992), Thresholds and the spatial variability of flood power during extreme floods, *Geomorphology*, *5*, 373–390, doi:10.1016/0169-555X(92)90014-F.

Magilligan, F. J., and B. E. Graber (1996), Hydroclimatological and geomorphic controls on the timing and spatial variability of floods in New England, USA, *J. Hydrol.*, *178*, 159–180, doi:10.1016/0022-1694(95)02807-2.

Magilligan, F. J., K. H. Nislow, G. B. Fisher, J. Wright, G. Mackey, and M. Laser (2008a), The geomorphic function and characteristics of large woody debris in low gradient rivers, coastal Maine, USA, *Geomorphology*, *97*, 467–482, doi:10.1016/j.geomorph.2007.08.016.

Magilligan, F. J., J. M. Kaste, C. E. Renshaw, G. B. Fisher, and K. H. Nislow (2008b), Application of fallout radionuclides as indicators of eco-geomorphic adjustments to dams, *Eos Trans. AGU*, *89*(53), Fall Meet. Suppl., Abstract H33B-1004.

Malmon, D. V., T. Dunne, and S. L. Reneau (2003), Stochastic theory of particle trajectories through alluvial valley floors, *J. Geol.*, *111*, 525–542, doi:10.1086/376764.

Manga, M., and J. W. Kirchner (2000), Stress partitioning in streams by large woody debris, *Water Resour. Res.*, *36*, 2373–2379, doi:10.1029/2000WR900153.

Manners, R. B., M. W. Doyle, and M. J. Small (2007), Structure and hydraulics of natural woody debris jams, *Water Resour. Res.*, *43*, W06432, doi:10.1029/2006WR004910.

Matisoff, G., C. G. Wilson, and P. J. Whiting (2005), The $^{7}Be/^{210}Pb_{xs}$ ratio as an indicator of suspended sediment age or fraction new sediment in suspension, *Earth Surf. Processes Landforms*, *30*, 1191–1201, doi:10.1002/esp.1270.

May, C. L., and R. E. Gresswell (2003), Processes and rates of sediment and wood accumulation in headwater streams of the Oregon Coast Range, USA, *Earth Surf. Processes Landforms*, *28*, 409–424, doi:10.1002/esp.450.

Montgomery, D. R. (1997), What's best on the banks?, *Nature*, *388*, 328–329, doi:10.1038/40976.

Montgomery, D. R., and J. M. Buffington (1997), Channel-reach morphology in mountain drainage basins, *Geol. Soc. Am. Bull.*, *109*, 596–611, doi:10.1130/0016-7606(1997)109<0596:CRMIMD>2.3.CO;2.

Montgomery, D. R., J. M. Buffington, R. D. Smith, K. M. Schmidt, and G. Pess (1995), Pool spacing in forest channels, *Water Resour. Res.*, *31*, 1097–1105, doi:10.1029/94WR03285.

Montgomery, D. R., B. D. Collins, J. M. Buffington, and T. B. Abbe (2003), Geomorphic effects of wood in rivers, in *The Ecology and Management of Wood in World Rivers*, edited by S. V. Gregory, K. L. Boyer, and A. M. Gurnell, *Am. Fish. Soc. Symp.*, *37*, 21–47.

Nistor, C. J., and M. Church (2005), Suspended sediment transport regime in a debris-flow gully on Vancouver Island, British Columbia, *Hydrol. Processes*, *19*, 861–885, doi:10.1002/hyp.5549.

Olsen, C. R., I. L. Larsen, P. D. Lowry, N. H. Cutshall, J. F. Todd, G. T. F. Wong, and W. H. Casey (1985), Atmospheric fluxes and marsh-soil inventories of ^{7}Be and ^{210}Pb, *J. Geophys. Res.*, *90*, 10,487–10,495, doi:10.1029/JD090iD06p10487.

Pyrce, R. S., and P. E. Ashmore (2003), The relation between particle path length distributions and channel morphology in gravel-bed streams: A synthesis, *Geomorphology*, *56*, 167–187, doi:10.1016/S0169-555X(03)00077-1.

Rathburn, S., and E. Wohl (2003), Predicting fine sediment dynamics along a pool-riffle mountain channel, *Geomorphology*, *55*, 111–124, doi:10.1016/S0169-555X(03)00135-1.

Salant, N. L., C. E. Renshaw, F. J. Magilligan, J. M. Kaste, K. H. Nislow, and A. M. Heimsath (2007), The use of short-lived radionuclides to quantify transitional bed material transport in a regulated river, *Earth Surf. Processes Landforms*, *32*, 509–524, doi:10.1002/esp.1414.

Schuett-Hames, D., A. E. Pleus, J. Ward, M. Fox, and J. Light (1999), TFW monitoring program method manual for the large woody debris survey, *Tech. Rep. TFW-AM9-99-004*, 33 pp., NW Indian Fish. Comm., Olympia, Wash.

Svendsen, K. M., C. E. Renshaw, F. J. Magilligan, K. H. Nislow, and J. M. Kaste (2009), Flow and sediment regimes at tributary junctions on a regulated river: Impact on sediment residence time and benthic macroinvertebrate communities, *Hydrol. Processes*, *23*, 284–296, doi:10.1002/hyp.7144.

Syvitski, J. P. M., C. J. Vörösmarty, A. J. Kettner, and P. Green (2005), Impact of humans on the flux of terrestrial sediment to the global coastal ocean, *Science*, *308*, 376–380, doi:10.1126/science.1109454.

Wallbrink, P. J., and A. S. Murray (1994), Fallout of ^{7}Be in south eastern Australia, *J. Environ. Radioact.*, *25*, 213–228, doi:10.1016/0265-931X(94)90074-4.

Wallbrink, P. J., and A. S. Murray (1996), Distribution and variability of ^{7}Be in soils under different surface cover conditions and its potential for describing soil redistribution processes, *Water Resour. Res.*, *32*, 467–476, doi:10.1029/95WR02973.

Walling, D. E., A. L. Collins, and R. W. Stroud (2008), Tracing suspended sediment and particulate phosphorous sources in catchments, *J. Hydrol.*, *350*, 274–289, doi:10.1016/j.jhydrol.2007.10.047.

Whiting, P. J., G. Matisoff, W. Fornes, and F. M. Soster (2005), Suspended sediment sources and transport distances in the Yellowstone River basin, *Geol. Soc. Am. Bull.*, *117*, 515–529, doi:10.1130/B25623.1.

Wohl, E., S. Madsen, and L. MacDonald (1997), Characteristics of log and clast bed-steps in step-pool streams of northwestern Montana, *Geomorphology*, *20*, 1–10, doi:10.1016/S0169-555X(97)00021-4.

Yarnell, S. M., J. F. Mount, and E. W. Larsen (2006), The influence of relative sediment supply on riverine habitat heterogeneity, *Geomorphology*, *80*, 310–324, doi:10.1016/j.geomorph.2006.03.005.

You, C. F., T. Lee, and Y. H. Li (1989), The partition of Be between soil and water, *Chem. Geol.*, *77*, 105–118, doi:10.1016/0009-2541(89)90136-8.

G. B. Fisher, Department of Earth Science, University of California, Santa Barbara, CA 93106, USA. (burch@crustal.ucsb.edu)

J. M. Kaste, Department of Geology, College of William and Mary, PO Box 8795, Williamsburg, VA 23187, USA.

F. J. Magilligan, Department of Geography, Dartmouth College, 6017 Fairchild Hall, Hanover, NH 03755, USA.

K. H. Nislow, Northern Research Station, U.S. Department of Agriculture, U.S. Forest Service, University of Massachusetts, Amherst, MA 01003, USA.